WILLIAM & MARY
CHARTERED 1693

Dissertations, Theses, and Masters Projects   Theses, Dissertations, & Master Projects

1996

Spectroscopic Characterization of Hg(II) Coordination Complexes

Sharon Rosemary Fitzhenry

College of William & Mary - Arts & Sciences

Follow this and additional works at: https://scholarworks.wm.edu/etd

Part of the Analytical Chemistry Commons

SPECTROSCOPIC CHARACTERIZATION OF
Hg (II) COORDINATION COMPLEXES

A Thesis

Presented to

The Faculty of the Department of Chemistry

The College of William and Mary in Virginia

In Partial Fulfillment

Of the Requirements for the Degree of

Master of Arts
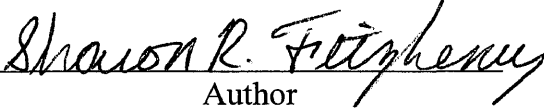
---

by

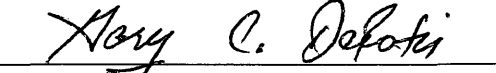Sharon R. Fitzhenry

1995

APPROVAL SHEET

This thesis is submitted in partial fulfillment of

the requirements for the degree of

Master of Arts

Sharon R. Fitzhenry
Author

Approved July 1995

Deborah C. Bebout
Deborah C. Bebout

Gary C. Defotis
Gary C. Defotis

Christopher J. Abelt
Christopher J. Abelt

ii

TABLE OF CONTENTS

ACKNOWLEDGEMENTS

LIST OF FIGURES

LIST OF TABLES

ABSTRACT

A series of nitrogen and sulfur containing organic molecules were designed to model metal coordinating enzyme active sites containing histidine and cysteine. Bis-2-(2-pyridylethyl) amine and tris-2-(2-pyridylethyl) amine, models of blue copper protein active sites, were successfully synthesized and purified. Work was begun on a third ligand, Di-(2-(2-pyridyl)ethyl) amino ethanethiol, and a ligand starting material, 2-(3-bromopropyl)pyridine.

Mercury (II) was used as a spectroscopic probe for these model complexes because of its favorable NMR properties and because its coordination preferences are similar to those of Cu (II). Bis-2-(2-pyridylethyl) amine, modeling a copper ligating active site of hemocyanin, was coordinated to Hg(II) and characterized by proton, carbon-13, and variable temperature NMR.

Continuation of this research is expected to yield a database of multinuclear NMR structure/spectroscopy relationships for known structures which may be applicable to spectra of compounds with unknown structures.

SPECTROSCOPIC CHARACTERIZATION OF

Hg (II) COORDINATION COMPLEXES

1

Introduction

We find ourselves in a bewildering world. We want
to make sense of what we see around us and to ask:
What is the nature of the universe? What is our
place in it and where did it and we come from?
Why is it the way it is? [1]

-Stephen W. Hawking

Most scientists spend their lives searching for answers to questions with a

narrower scope, hoping to uncover truths that will come together to answer these broader

questions. Science is a cumulative field where the ideas and research of an individual

come together with those of their peers and predecessors to resolve questions raised in the

search for a heightened understanding of our world and ourselves.

Essential to enhancing our understanding of ourselves is increasing our knowledge of the mechanism by which proteins catalyze biochemical reactions. The goal of the ongoing research presented herein is to synthesize a series of multidentate ligands (Figure 1.1), modeling the amino acid ligation of enzyme active sites, and to characterize the effect of Hg (II) binding on their ^{1}H NMR. Our research will establish structure/ spectroscopy relationships applicable to protein bound mercury.

Bis-2-(2-Pyridylethyl)amine   Tris-2-(2-Pyridylethyl)amine

Di-(2-(2-pyridyl)ethyl)amino   ethanethiol

Figure 1.1 Series of Multidentate Ligands Designed for Study

Essential to enhancing our understanding of ourselves is increasing our

knowledge of the mechanism by which proteins catalyze biochemical reactions. The goal

of the ongoing research presented herein is to synthesize a series of multidentate ligands

(Figure 1.1), modeling the amino acid ligation of enzyme active sites, and to characterize

the effect of Hg (II) binding on their ^{1}H NMR. Our research will establish structure/

spectroscopy relationships applicable to protein bound mercury.

Bis-2-(2-Pyridylethyl)amine   Tris-2-(2-Pyridylethyl)amine

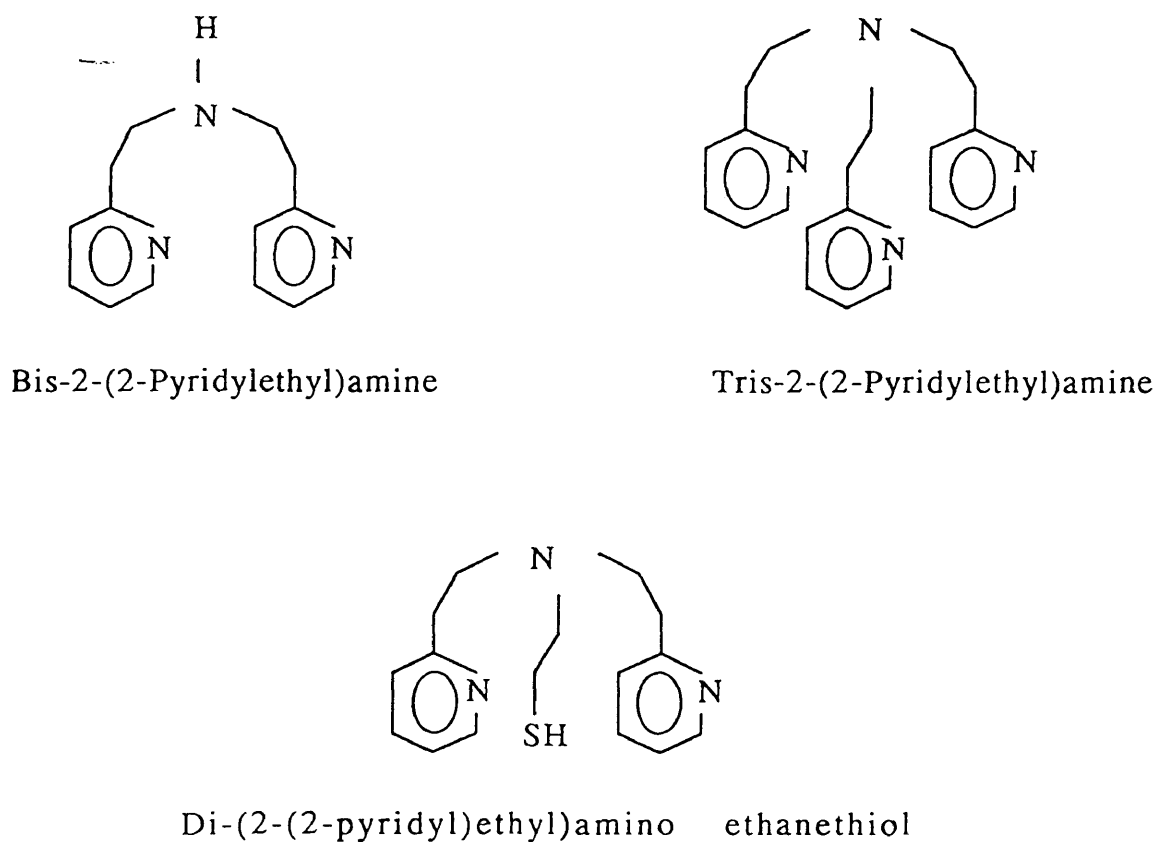Di-(2-(2-pyridyl)ethyl)amino   ethanethiol

**Figure 1.1 Series of Multidentate Ligands Designed for
Study**

The areas that scientists choose to work on are often so complex that it is necessary to start with model systems that theoretically approximate the behavior or some facet of the behavior of the system being studied. This is the case with research on the interactions of metals, in our case mercury, on metalloenzymes. By simplifying the problem, model systems enable researchers to study phenomena that occur in nature but which are obscured by the complexity of biological systems.

The series of ligands was designed to approximate only the active sites of metalloenzymes containing histidine, cysteine, and methionine residues. Theoretically, this series should possess many characteristics attributable to the enzymes. The pyridine rings are structurally analogous to histidine functional groups while the thiol side chain is similar to cysteine residues. Because of the structural similarity between the amino acid donor groups and the ligand donor groups, theoretically the ligands will model the behavior of the amino acids. While imidazole is more structurally analogous to histidine, it was not used as a model because it is more reactive than pyridine. This would have further complicated the synthetic chemistry.

Another advantage to the series chosen is that varying the length of the carbon bridge between the central amine nitrogen and the pyridine or thiol functional groups, in future studies, will provide increasing flexibility in the three dimensional structures. This design increases the number of allowable conformations, thereby approximating a greater number of native tertiary structures. By beginning with simple systems and expanding to

larger systems we should be able to deconvolute the complex issue of how chemical environment affects the nuclear magnetic resonance shifts for Proton, Carbon-13, and Mercury-199 spectroscopy at room temperature and at low temperatures.

In biosystems, enzyme active sites are subject to replacement of the native metal cofactor by other metal ions;[2] an example of which is replacement of Zn (II) by Hg (II) ions in Human Carbonic Anhydrase B.[3] As one would expect, this can distort the native conformation of the enzyme in some cases destroying their catalytic activity. In addition to its toxic effects, Hg (II) also has the detrimental quality of being bioaccumulative since few organisms have developed an effective mechanism for ridding it from the body.[3,4]

NMR Spectroscopy has been described as "the most powerful spectroscopic tool in chemistry today".[5] Its applications transcend the boundaries of organic, inorganic, and biological chemistry--all fields applicable to the study and manipulation of proteins. A brief overview of the theory behind various spectroscopic techniques is present in Appendix A. In addition to its more commonly used proton and carbon-13 capabilities, NMR spectroscopy can also be applied to exploration of ^{199}Hg nuclei. ^{199}Hg has a spin quantum number equal to 1/2 and isotopic abundance of 16.84%,[6] making it an accessible nucleus for this type of spectroscopy. Detailed structural information from NMR is only possible with nuclei having half-integer spin quantum numbers and a high relative abundance gives rise to strong signals. Mercury-199 has a receptivity 5.4 times greater

than that of carbon-13 and therefore gives a stronger signal. Hydrogen has an extremely high natural abundance, so it gives the strongest signal.

Variable temperature is especially beneficial when it is necessary to decrease the kinetic energy available for ligand-metal exchange in order to make the ligand/Hg complex stable on an NMR time scale. In some cases, rapid ligand exchange at room temperature prevents separate NMR characterization of bound and free ligand. Rather than reporting peaks for ligand/Hg complexes and unbound ligand separately, it reports a molar weighted average of these values.[7]

While X-ray crystallography is a well respected means of structural determination, NMR spectroscopy offers some advantages not available through X-ray techniques. In living systems, most proteins exist in solution and crystallization can distort their native conformation. [8] NMR experiments are conducted in solution, therefore more closely approximating a cell-like environment. Information gained should be more representative of the *in vivo* structure of the metalloprotein; thus supplementing existing x-ray data.

This study is intended to evaluate the applicability of NMR technology to the study of multidentate chelates of Hg(II). It is our expectation that the data resulting from this study and continuation of the work will be of direct use in future studies of mercury bound enzymes.

2

Experimental

I. INTRODUCTION

The first step in synthesizing ligand/Hg complexes was synthesis of ligands and ligand starting materials. Thus far, two ligands have been synthesized and positively identified. Work was begun on a third ligand and a ligand starting material, which await purification and positive identification.

To simplify the text, the rest of this chapter introduction explains elements of research that remained constant. The remainder of the chapter is devoted to the experimental procedures followed by the results of procedures and a discussion of these results.

A. Starting Materials

Table 2.1 and 2.2 give important physical constants for starting materials for the organic syntheses and the metal coordinations respectively. They also contain a reference page number for Appendix B where NMR, GC, and MS data appear. They appear in the order that they appear in the text. Abbreviations, which will be used hereafter, are defined and used for the first time.

Table 2.1 Starting Materials for Organic Compounds

Starting Material	MW	ρ (g/ml)	Spectra
2-Vinylpyridine (2VP)	105.14	0.975	
2-(2-Aminoethyl)pyridine (AEP)	122.17	1.021	
Ammonium Acetate (AA)	77.08		
Glacial Acetic Acid (GAA)	60.05	1.049	
Methanol (MeOH)	32.04	0.791	
Bis-(2,2-Pyridylethyl)amine(N3)	227.31		54-55
Ethylene Sulfide (EtS)	60.12	1.010	
Benzene	78.11	0.874	
2-(3-Hydroxypropyl)pyridine (HPP)	137.18		56-57
Triphenyl phospine (TPP)	262.29		
N-Bromosuccinimide (NBS)	177.99		
Tetrahydrofuran (THF)	72.11		

Table 2.2 Starting Materials for
Metal Coordination Complexes

Starting Material	MW (g/mol)	ρ (g/ml)	Spectrum
N3	227.31		54-55
Mercury (II) oxide (HgO)		216.59	
Perchloric acid (HClO4) (68%)		1.694	
Deionized water (H2O)	18.0	1.000	
Mercury (II) iodide (HgI2)	454.20		
Flouroboric acid (HBF3) (30%)			

B. Analytical Instruments

All NMR spectra were obtained on a General Electric QE-300 NMR spectrometer

operated by a CHARM software program. The instrument was originally purchased from

a division of General Electric which has since come under the management of Bruker.

The gas chromatographic/mass spectral data was obtained using an HP-5890

Hewlett Packard gas chromatographer in conjunction with a mass spectrometer.

Three temperature methods were developed for GC/MS as shown in Table 2.3,

2.4, and 2.5. Method DCB1.M (Table 2.3) was used for elution of N3 and N4. The

method in Table 2.4 was created for N3S, but has since been deleted. Method DCB2.M

(Table 2.5) was developed for elution of HPP and BPP.

Table 2.3 Method Parameters for DCB1.M
Elution of N3 and N4

Temperatures (°C)		Other Parameters	
Injector B	280	Equilibration time	0.50 min
Detector B	245	Time at init. temp.	2.00 min
Initial	150	Rate/Minute increase	10.0 °C
Final	250	Time at final temp.	8.00 min

Table 2.4 Method Parameters for
Elution of N3S

Temperatures (°C)		Other Parameters	
Injector B	250	Equilibration time	0.50 min
Detector B	250	Time at init. temp.	10.00 min
Initial	220	Rate/Minute increase	12.0 °C
Final	280	Time at final temp.	15.00 min

Table 2.5 Method Parameters for DCB2.M
Elution of HPP, BPP

Temperatures (°C)		Other Parameters	
Injector B	250	Equilibration time	0.50 min
Detector B	245	Time at init. temp.	2.00 min
Initial	100	Rate/Minute increase	10.0 °C
Final	250	Time at final temp.	5.00 min

C. Hazardous Waste Procedures

All hazardous organic and halogenated waste was disposed of in separate

hazardous waste bottles stored in the fume hood. When hazardous halogenated waste

was rotovapped, the aspirator trap flask was immersed in an acetone bath which was cooled to -60 °C by a Neslab CC-65-II Cryotrol. The halogenated waste condensed in the flask and was promptly disposed of in the designated waste bottle. All heavy metal and acid waste was also disposed of in a specially designated waste bottle stored under the hood.

D. Glassware and General Procedures

Round-bottom flasks, reflux columns, distillation heads, distillation cows, and pressure tubes were oven dried at temperatures in excess of 100 °C for 24 or more hours before use. The glassware was removed from the oven just prior to the reaction, assembled immediately in the fume hood, and septa were placed over any openings to the atmosphere. The apparatus was then flushed with nitrogen by inserting syringe needles through the septa and allowing air from a nitrogen tank to flow through the apparatus. While the apparatus was being flushed with nitrogen, it was dried with a heat gun.

For reactions involving a reflux column or a distillation apparatus, the column or apparatus was attached to a "dummy" round-bottom flask first so that the reactants could be added more easily to the reaction flask. Syringes were used to add all liquid reagents through the septa. After the reagents had been added, the reflux tube or distillation apparatus was attached to the reaction vessel and the assembled apparatus was flushed for

another ten minutes. It was then placed under positive pressure and the condenser water was started. All joints were greased with heat resistant lubriseal.

For reactions involving pressure tubes, solid reagents were added first by removing the septum, adding the reagent, then replacing the septum and flushing the tube with nitrogen for an additional five minutes. Liquid reagents were added via syringe. After the reagents were added the tubes were flushed for between five and 45 minutes, the Teflon covers were screwed on, and they were placed in preheated mineral or silicon oil baths. When reaction progress was monitored invasively by NMR, the apparatus was flushed with nitrogen again before continuing the reaction.

E. Flash Chromatography

Flash chromatography[1] is a chromatographic technique developed for rapid separation and elution of reaction products. The narrow glass channel just above the stopcock of a standard chromatographic column was plugged with glass wool (not too tightly). An eight of an inch of clean sand was added on top of this, making sure the top of the sand was flat. According to the procedure, 5.5 to 6 inches of silica or alimina gel is poured on top of the sand. In our procedure, 10.5 inches of silica gave a better separation. On top of the silica another eigth of an inch of sand was poured. The top of both the silica and the sand were flat. The solvent was then added to the column, making sure the stopcock was open, so that any air was forced out of the column. When the column was

filled with solvent, the solvent was forced through under pressure of nitrogen in order to pack the column. (The column is ready when it becomes uniform gray in color.)

Once the column was packed, a flow rate of nitrogen that gave a solvent flow rate of 2 ml/min was established. The level of solvent was lowered to just above the sand but above the silica. The sample was then loaded via syringe directly onto the sand and the stopcock was opened long enough to allow the sample to drain onto the silica, but the silica was not exposed to the air. Solvent was then added carefully to the top and the system was placed under the pre-established nitrogen flow. Fractions were collected in test tubes and monitored by TLC. When the fractions no longer stained by iodine, the chromatography was concluded.

II. ORGANIC COMPOUNDS

A. Bis-2-(2-pyridylethyl)amine (N3)

Each synthesis of N3[2] was carried out in a similar manner using varying quantities of reactants. Highest yield (24.9 %) was obtained when 2.70 ml of distilled 2VP (25 mmols; b.p. 59 °C, 22.5 mm Hg) was added to a solution of 3.00 ml of distilled AEP (25 mmols; b.p.104 °C, 22.5 mm Hg), 1.43 ml of glacial acetic acid, and 50 ml of methanol in a round-bottom flask. The mixture was then allowed to reflux for 24 hours using a mantle as a heat source.

After the flask cooled, the methanol was removed by rotary evaporation and the

yellow, oily residue was neutralized with 10 M sodium hydroxide to a pH of about 9.

The amine was extracted using 4x10 ml portions of chloroform. The combined extracts

were dried over $MgSO_4$, filtered into a round-bottom flask, and the solvent was removed

under reduced pressure. The solvent was discarded and the product was distilled.

The product was purified by vacuum distillation at 133 °C and 0.35 mm of Hg.

Pure product (1.4161 g, 6.23 x 10^{-3}) was isolated giving a yield of 24.9 %. The distilled

product was a clear, viscous liquid. ^{1}H NMR (chloroform-d) (page 54): δ 2.99 (t, J=12

Hz, 2 H), 3.08 (t, J=12 Hz, 2H), 7.10 (t, J=12 Hz, 1H), 7.14 (d, 1H), 7.56 (t, J=12 Hz,1

H), 8.48 (d, 1H). ^{13}C NMR (Chloroform-d) (page 54): δ 38.45, 49.25, 121.12, 123.22,

136.28, 149.26. GC/MS: (rel int) 227 (M+, 3921), 135 (211,517), 121 (32, 855), 107

(28, 869), 106 (205, 312), 94 (62, 113), 93 (102, 790), 79 (36, 312), 78 (77, 113), 65

(37,894), 51 (29, 138), 39 (27, 515), 28 (13, 532).

B. Tris-2-(2-pyridylethyl)amine (N4)[3]

Presented in this section is the experimental procedure for Trial 14 of the N4

syntheses which yielded the highest amount of product (23.1 %). Many different

experiments, summarized in the Results and Discussion chapter, were carried out in an

attempt to optimize the yield and purity of the synthesis.

Trial 14 yielded the highest percent of purified product. 2VP (1.25 ml, 11.6 mmols) was added to ammonium acetate (0.15 g, 1.96 mmols) in a 15 ml pressure tube with a Teflon screw cap. The reaction was begun with approximately 0.5 ml of MeOH and approximately 0.5 ml more was added throughout the course of the reaction to wash down sublimed ammonium acetate.

The tube was immersed in a silicon oil bath heated with a nichrome resistance wire encased in glass and controlled by a Variac. The temperature of the bath was approximately 105 °C. The mixture was allowed to react for 3 days before it was removed from heat.

Because the quantity of solvent was so small, it was not rotovapped off. Product was isolated from the cooled reaction mixture by the method of Chi-Ming Che and coworkers.[4] The mixture was neutralized to a pH of about 9 using 10 M NaOH. About 10 ml of methylene chloride was added to the brown reaction mixture to dissolve the product. The mixture was poured into a separatory funnel and was extracted with 4 x 15 ml portions of dichloromethane in a 60 ml separatory funnel. The combined extracts were dried over magnesium sulfate and filtered through filter paper into a round-bottom flask. The dichloromethane was removed by rotary evaporation.

The products of the reaction were separated by flash chromatography using a 40 mm column with 10.5 inches of silica gel. Methanol was used as eluant. Fractions (20

ml per fraction) were collected and individually analyzed by thin layer chromatography. Methanol was used to develop the plates and they were stained with iodine. (Rf= 0.11)

Similar fractions were combined in round bottom flasks and nitrogen was bubbled through them if they were going to be stored for any period of time. The methanol was rotovapped off, taking great care to ensure that the product was not exposed to the atmosphere for long periods of time. ^{1}H NMR (chloroform-d) (page 57): δ 2.92 (q, J=15 Hz, 2 H), 3.00 (q, J=15 Hz, 2H), 7.03 (t, 1H), 7.09 (d, J=12 Hz, 1H), 7.53 (t, J=18 Hz, 1H), 8.50 (d, 1H). ^{13}C NMR (Chloroform-d) (page 57): δ 36.19, 54.10, 121.19, 123.62, 136.24, 149.35, 160.81. GC/MS: (rel int) 332 (M+, 192), 240 (11,575), 226 (620), 147 (7313), 135 (15,393), 106 (27,688), 93 (5039), 79 (3521), 78 (8487), 65 (2312), 16 (1363), 14 (2700).

C. Di-(2-(-2-pyridyl)ethyl)amino ethanethiol (N3S)

Synthesis of this compound was attempted following the general guidelines of an analogous synthesis.[5] A summary of reaction conditions appears in Table 2.6. Spectral comparison permitted preliminary characterization of N3S. The synthesis procedure for the most promising reaction, Trial 2, is detailed below.

Table 2.6 N3S Experimental Reaction Conditions

Trial	N3	N3 (mols x 10^{-4})	EtS (g)	EtS (mols x 10^{-4})	Benzene (ml)	Time (hrs)	Ratio N3:EtS: Benzene
1	0.079	3.47	0.025	4.20	0.04	1	1:1.2:1.3
2	0.099	4.35	0.026	4.36	0.05	5	1:1:1.3
3	0.158	6.95	0.050	8.34	0.08	17	1:1.2:1.3

For Trial 2, N3 (99 mg, 0.347 mmols) of and 0.05 ml benzene were combined in a 15 ml pressure tube with a magnetic stir bar and immersed in an ice bath. Ethylene sulfide (0.026 +/- 0.002 ml, 4.36 x 10^{-4} mols) was added via syringe and the cap for the pressure tube was put in place.

The pressure tube was transferred to a silicon oil bath, heated by a hot plate, which varied in temperature from 80 to 130 °C. It was allowed to react for 5 hrs and then it was removed and allowed to cool. The tube was flushed with a rapid flow of nitrogen to remove any unreacted ethylene sulfide.

D. 2-(3-bromopropyl)pyridine

Recrystallization of N-Bromosuccinimide:[6]

Pale yellow NBS crystals (30 g, 0.169 mols) were added to 300 ml of boiling deionized water. The orange solution was stirred by hand with a glass rod for 15 minutes, until all of the crystals had dissolved. The hot solution was filtered into an Erlenmeyer

flask submerged in an ice bath in four portions to reduce loss from crystallization on the filter paper. The remaining solution was kept warm then filtered when the funnel drained. A white solid crystallized from the orange liquid.

The mixture was kept in the ice bath for two hours and then the crystals were collected by vacuum filtration. The NBS was washed with water and kept under suction for 15 minutes. The white crystals were dried overnight in a vacuum desiccator. Yield: 24.69 g (0.139 mols, 82.2%).

Distillation of 2-(3-Hydroxypropyl)pyridine:

Commercially available HPP was distilled at 72 °C under a vacuum of 0.02 mm of Hg (lit bp 190-195 °C, 20 mm Hg) to provide a colorless liquid.

Synthesis:

The synthesis procedure for this molecule followed the guidelines of a general bromination reaction.[7] Various reaction conditions are summarized in Table 2.7. Results looked most promising for the third trial, in which purified NBS and HPP were used. (In Trial 1, no starting materials were purified; in Trial 2, the only purified starting material was HPP.)

Table 2.7 BPP Experimental Conditions

Trial	NBS (g)	TPP (g)	HPP (g)	THF (ml)	Ratio (NBS:TPP:HPP)
1	1.3535	1.9968	1.0439	10	1:1:1
2	1.4346	2.1121	1.1049	13	1:1:1
3	1.3503	1.9902	1.0409	10.5	1:1:1

Recrystallized NBS (1.35 g, 7.59 mmols) was added to a preflushed 25 ml round-bottom flask. The NBS was dissolved in 6 ml of dry THF. Though the crystals were white, the solution was orange-red, perhaps due to occluded bromine. The 25 ml flask was submerged in an ice bath.

TPP (1.99 g, 7.59 mmols) was dissolved in 3 ml of dry THF. The solution was added dropwise via syringe to the NBS/THF in the flask. The orange color disappeared gradually and a white precipitate formed. At some point the magnetic stir bar became embedded in the solid so another one was added on top of it.

After 1 hour, the solution was removed from the ice bath. A mixture of distilled HPP (1.04 g, 7.59 mmols) and dry THF (1.0 ml) was added dropwise via syringe. The syringe was rinsed with 0.5 ml of THF, which was added to the reaction mixture. No visible changes in type, amount, or color of the solid occurred. After another hour, the

solid had still not dissolved as was expected so the reaction was assumed to be finished. It was stoppered and placed in the freezer overnight.

The reaction mixture was rotovapped to remove the THF and the reaction mixture was extracted with ether/water to remove TPP into the ether layer. Salt was then added to the water layer and the crude BPP was extracted from the brine solution with chloroform. The chloroform was then rotovapped off.

III. Metal Ligation

After the N3 ligand was successfully synthesized, it was possible to begin synthesis of coordination complexes. Two factors were of interest in synthesis and study of these complexes: (1) determining the ratio of ligand to metal which would favor a stable ligand/Hg complex, and (2) discovering which counterion increased stability of the ligand/Hg complex.

All reactions were carried out following general procedures outlined in an article by G. Cova, et al. Physical constants for starting materials appear in Table 2.2. Spectral data for N3 appears on pages 54 and 55 in Appendix B.

A. (N3)x•Hg(II)•(ClO4)2 [X= 1-3]

This complex was synthesized following a general procedure for synthesizing

coordination complexes using perchlorate counterions. A 3 to 1 ligand to mercury ratio

was used in this synthesis. HgO (0.03001 g, 0.138 mmols) was dissolved in a solution of

0.10 ml of HClO4 in 0.30 ml of H2O using a magnetic stir bar. N3 (0.09672 g, 0.426

mmols) was added dropwise via syringe. A white solid precipitated immediately.

The white precipitate was collected in a Hirsch funnel by vacuum filtration. The

crystals were washed with 5 ml of cold, deionized water and 5 ml of cold, absolute

ethanol. Air was pulled through for an additional 10 minutes to help dry the crystals.

The isolated crystals were soluble in acetonitrile and acetone. The crystals were further

dried for 5 minutes at 10^{-3} mm Hg. They were dissolved in acetone for spectroscopic

study. ^{1}H NMR (acetone-d6) page 63):   δ 3.43 (t, 2H), 3.81 (t, 2H), 7.41-7.49 (m, 2H),

7.88 (q, 1H), 8.57 (d, 1H). ^{13}C NMR (acetone-d6) (page 63): δ 37.96, 49.37, 126.52,

129.11, 144.20, 151.44, 160.30.

B. N3x•Hg (II)•I2 [X=1-3]

HgI2 (65.1 mg, 0.14 mmols) of was dissolved in a solution of 1 ml of deionized

water and 4 drops of HI using a magnetic stir bar. N3 (95.73 mg, 4.2 mmols) was added

dropwise and a yellow crystal precipitated.

The precipitate was collected in a Hirsch funnel and washed with cold, deionized water followed by cold chloroform. The crystals were then placed in a round-bottom flask and vacuum dried for 5 minutes at 10^{-3} mm Hg. They were dissolved first in deuteroacetonitrile then in deuteracetone for spectroscopic study. ^{1}H NMR (acetone-d6) (page64): δ 3.34 (t, 2H), 3.57 (t, 2H), 7.50 (d, 1H), 7.53 (d, 1H), 7.99 (t, 1H), 8.53 (d, 1H). ^{13}C NMR (page 64): 31.88, 47.71, 124.24, 125.59, 140.34, 149.26, 160.21.

C. N3x•Hg•(BF3)2 [x=1-3]

Red mercuric oxide crystals (44.8 mg, 0.21 mmols) were dissolved in 0.25 ml of HBF3 and 0.25 ml of deionized water, stirred magnetic stir bar. N3 (0.10 ml, ~4.2 x 10^{-4} mmls) was added dropwise via syringe to the clear solution. No precipitate was observed so an additional 0.10 ml of N3 was added. Still no solid precipitated, even after the reaction vessel was submerged in an ice bath. The reaction was discarded.

III. VARIABLE TEMPERATURE NMR STUDIES

N3x•Hg (II)•(ClO4)2 and N3x•Hg (II) • I2 [x=1-3] were studied by variable temperature NMR. Experiments were performed at temperatures ranging from -90° C to 20.0° C in increments not greater than 20 degrees. Deuteroacetone was used as a solvent in the experiments presented because of its low freezing point (< 90° C).

3

Results and Discussion

I. ORGANIC COMPOUNDS

A. Bis-2-(2-Pyridylethyl)amine

The synthesis of N3 involves the nucleophilic attack of the 2VP olefin bond by

AEP, forming a secondary amine (Figure 3.1). Data collected for this compound

indicates that it was successfully synthesized. The number of peaks, integration

constants, and splitting patterns for the proton spectrum, page 54, agree with theory as

well as literature values reported in the original research article.[1] While ^{13}C values

were not reported, assignments can be made for the seven peaks appearing in our

spectrum, page 54, based on equations and constants found in literature sources.[2,3]

H
|
N

NH₂   +

AEP   2VP   N3
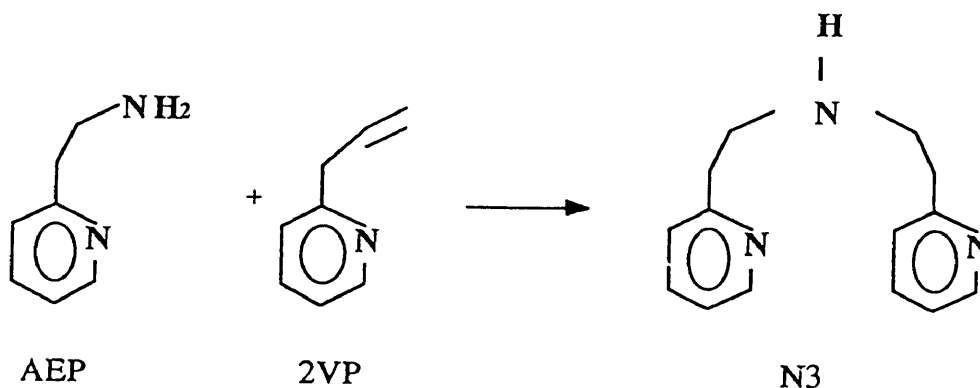
Figure 3.1 Reaction forming N3

The GC trace and mass spectrum are located on page 55. The m/z value for the

molecular ion was 227 which corresponds to the molecular weight of N3. Fragment ions

shown on the mass spectrum were attributable to various fragments of the N3 molecule.

The yield of 24.9 % was somewhat less than the 39 % yield of the original

researchers. Their reaction was run at approximately 4 times the scale of ours, so less

was probably lost during transfer and distillation.

B. Tris-(2-(2-Pyridylethyl)amine

N4 proved to be a difficult molecule both to synthesize and purify. The reaction

involves a nucleophilic addition of $^+$NH₄ accross the vinyl bond of three 2VP molecules,

generating a tertiary amine (Figure 3.2).[4]
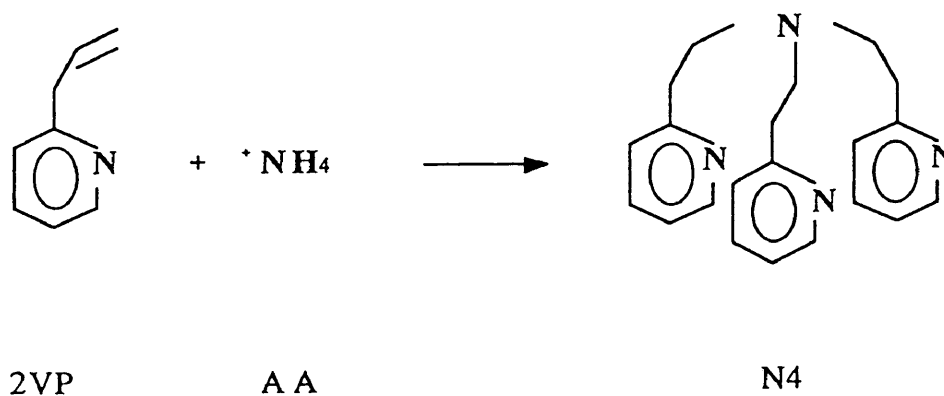
Figure 3.2 Reaction forming N4

Surprisingly, no formation of N3 or AEP was evident in the NMR spectra taken to monitor this reaction. Formation of these species would have been identified most clearly in the alkyl region of the spectrum where N3 has triplets at 2.99 and 3.08 and AEP has triplets at 2.92 and 3.11. No matching peaks were evident in any of the reactions.

Table 3.1 lists the various conditions of experimentation in an attempt to optimize synthesis of this molecule.

Table 3.1 N4 Experiments

Trial	Ratio 2VP:AA	Temp. °C	Time (hrs)	% Yield
0	5:1 then 10:1	65	24 hrs then 24 more hrs	none
1	1:1	65	48	none
2	2:1	65	48	2.2
3	1:1	65	48	none
4	2:1	65	48	8.64
5	8:1	65	48	none
6	8:1	70	48	none
7	5:1	70	240	none
8	6:1	130	50	none
9	6:1	130	24	none
10	~3:1	80-120	60	21.7
11	6:1	110	48	4.36
12	6:1	130-140	91	none
13	6:1	135	48	none
14	6:1	104-106	72	23.1
15	6:1	104-106	72	
16	6:1	80-90	360	not able to purify
17	6:1	100	206	not able to purify
18	6:1	split after 410 hrs		27.09
18A	6:1	80	410	
18B	6:1	80		
19	6:1	80	240	not able to purify

N4 was contained in the later fractions collected during column chromatography.

The proton and carbon spectra are located on page 58. The proton data is comparable to

literature values.[5] Carbon values are similar to those for N3 and are comparable to values calculated from literature sources.

GC/MS data further corroborates the identity of N4. The GC trace and mass spectrum, and area percent report are located on page 59. The mass spectrum shows an $m/z=332$ which corresponds to the molecular weight of N4. Molecular ions shown on the mass spectrum were attributable to various fragments of the N4 molecule.

C. Di-(2-(2-pyridyl)ethyl) amino ethanethiol

Data suggests, but does not confirm, synthesis of the N3S molecule in Trial 2. The synthesis (Figure 3.3) would proceed by nucleophilic attack of an amine on an episulfide-ethylene sulfide.

Proton and carbon data, page 60, are consistent with product formation, as will be discussed. GC/MS analysis of the reaction mixture did not reveal a component with a molecular ion with m/z 287, the molecular weight of N3S (page 61). However, only N3 starting material was observed by GC/MS. This may be explained by the fact that extremely polar molecules, like this sulfur/nitrogen containing molecule, are relatively nonvolatile and may adsorb strongly to the column.
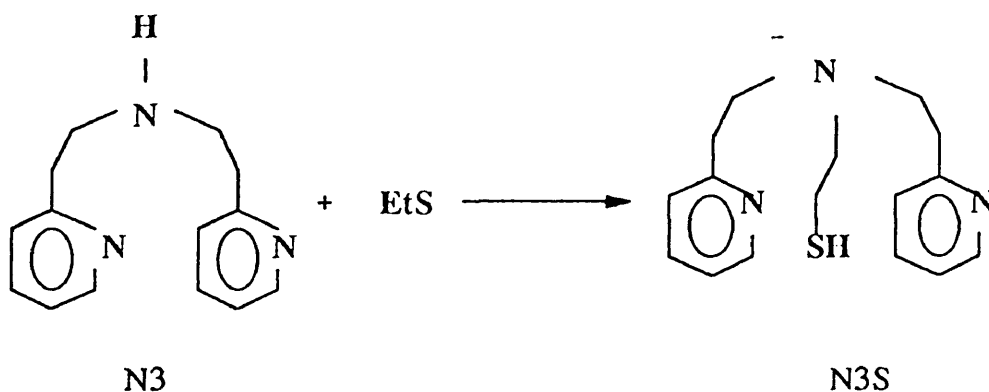
Figure 3.3 Synthesis of N3S

The proton spectrum for the reaction mixture is located on page 60. While the alkyl and aryl regions are difficult to interpret, integration constants, summarized below in Table 3.2, show that the hydrogens are in a ratio of approximately 1 Ar:1 Ar: 2 Ar: >6 Alk. N3S would exhibit a 1:1:2:6 ratio, but in this case, contribution from N3 starting material lowers the integration value for the alkyl region. The ^{1}H data is further supported by the ^{13}C spectrum, p. 60, which has 16 peaks--seven of which belong to N3. They are summarized in Table 3.3. N3S contains 9 chemically different carbons which can reasonably be assigned to the remaining peaks.

Table 3.2 Summary of Proton NMR Data for N3S

Peak Region	# of Protons
2.47-2.92	~5.5
6.82-6.98	2
7.29-7.40	1
8.26-8.30	1

Table 3.3 Summary of Carbon-13 Data for N3S Reaction II

Resonances	N3 Resonances	Remaining Resonances
36.15		36.15
36.83		36.83
37.95	38.45	
49.14	49.25	
53.61		53.61
54.13		54.13
121.34	121.12	
121.49		121.49
123.54	123.22	
123.71		123.71
136.45	136.58	
136.74		136.74
149.23	149.26	
149.37		149.37
160.07		160.07
160.51	160.21	

While this evidence is not conclusive, it is encouraging. The next step in the study of this molecule should be addition of a methyl group to the thiol functionality-using the guidelines of similar alkylations. This will make the molecule less polar and

therefore easier to work with during purification by column chromatography and analysis by GC/MS.

D. 2-(3-Bromopropyl)pyridine

The halogenation of HPP (Figure 3.4) proceeds by S_N2 replacement of the hydroxyl group by bromine.

TPP   NBS   TPPBr   Succinimide

HPP   TPPBr   BPP   TPP Oxide
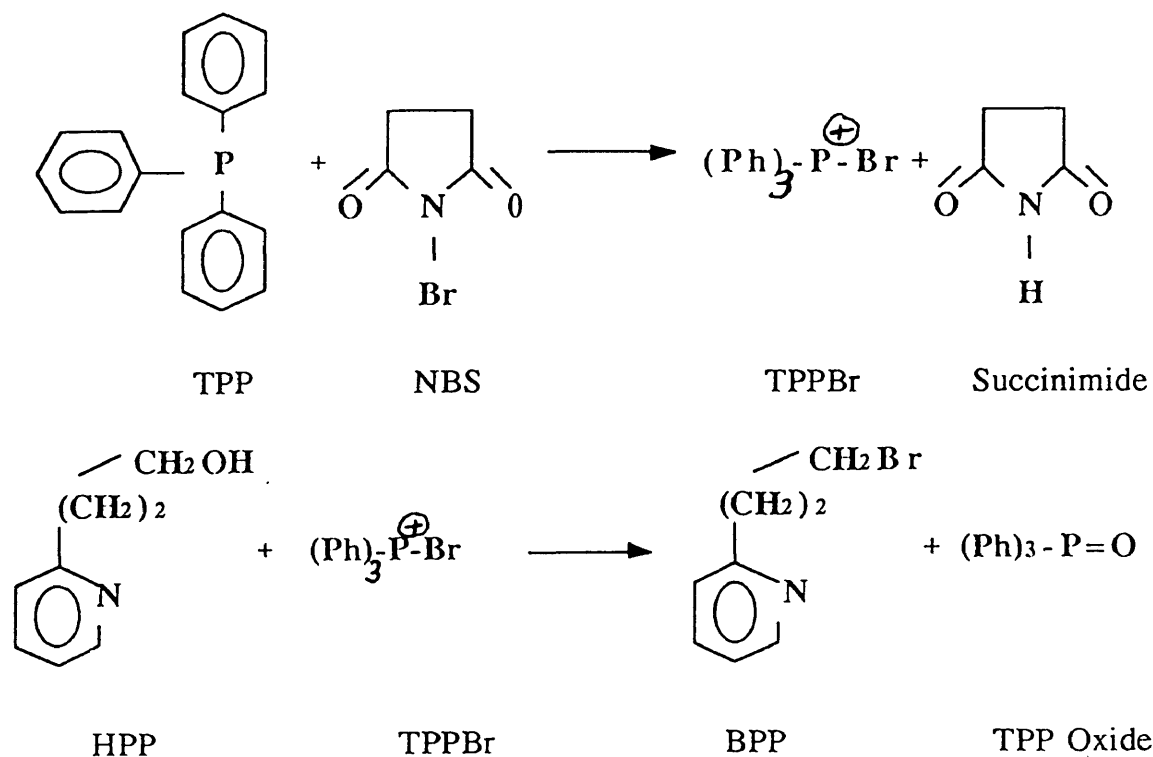
Figure 3.4 Synthesis of BPP

Comparison of the NMR spectrum for the chloroform layer of Trial 3 (page 62) with a spectrum for pure starting material, HPP (page 56), indicated product formation.

Below, Table 3.4 summarizes the peaks for both alkyl regions and also gives integrated peak area ratios.

Table 3.4 HPP vs. BPP Synthesis NMR Alkyl Regions

HPP Peaks	# Protons	BPP Syn. Peaks	# Protons
1.99 quint.	1	1.99 quint.	2
		2.26 quint.	0.5
		2.50 t	0.5
2.92 t	1	2.97 t	2
3.69 t	1	3.70 t	2
		4.35 t	0.5

There was peak formation in the alkyl region with splitting patterns consistent with a brominated propyl chain. The data is consistent with 0.20 mol fraction (0.5/2.5) BPP production based on integration constants for the alkyl region. No weight was measured so an approximate yield is not available.

GC/MS data (shown on page 63) was inconclusive and only starting material (shown on page 57) eluted in large quantity. Because HPP and BPP are much more volatile than N3 and N4, method DCB2.M was written and used to elute this compound. The method uses lower temperatures.

TLC was performed on silica with methanol but both HPP starting material and the BPP reaction mixture gave a single spot of Rf=0.708. So, while formation of this compound is promising, separation may prove more difficult. Future efforts to synthesize

this compound should focus on optimizing conversion of HPP to BPP to simplify

purification.

II. METAL LIGATION RESULTS

A. N3x•Hg(II)•(ClO4)2 [X=1-3]

N3x•Hg(II)•(ClO4)2 [X=1-3] (Reaction 3.1) was the most promising N3/Hg

complex because its proton NMR peaks (p. 64) were shifted furthest downfield from

those of pure N3 ligand. Table 3.5 summarizes ^{1}H and ^{13}C resonances (p. 64) for N3 vs.

N3x•Hg(II)•(ClO4)2 [X=1-3] and is followed by a graph (Figure 3.5) illustrating the

change in resonance between bound and unbound ligand. In all graphs, series one (x)

represents N3 peaks while series two (♦) represents Hg bound ligand. In general,

coordination to Hg (II) would cause a shift downfield because the positively charged

mercury ion is withdraws electron density from neighboring nuclei (see Appendix A).

$$3 \text{ N3 } + \text{HgO } + \text{ 2 HClO4 } \rightarrow \text{N3x•Hg(II)•(ClO4)2} + \text{ H2O } \quad (3.1)$$
$$[\text{X=1-3}]$$
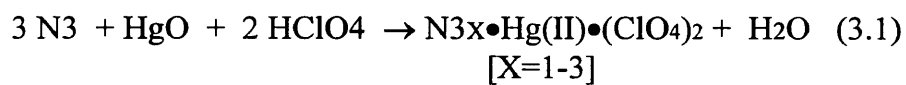
**Table 3.5 Proton Spectra of N3x•Hg(II)•(ClO4)2 [X=1-3]
vs. N3**

N3•Hg•(ClO4)2 ppm	N3 ppm	Δ ppm (N3Hg-N3)
3.43	2.99	0.44
3.81	3.08	0.73
7.41	7.10	0.31
7.49	7.14	0.35
7.88	7.56	0.32
8.57	8.48	0.09
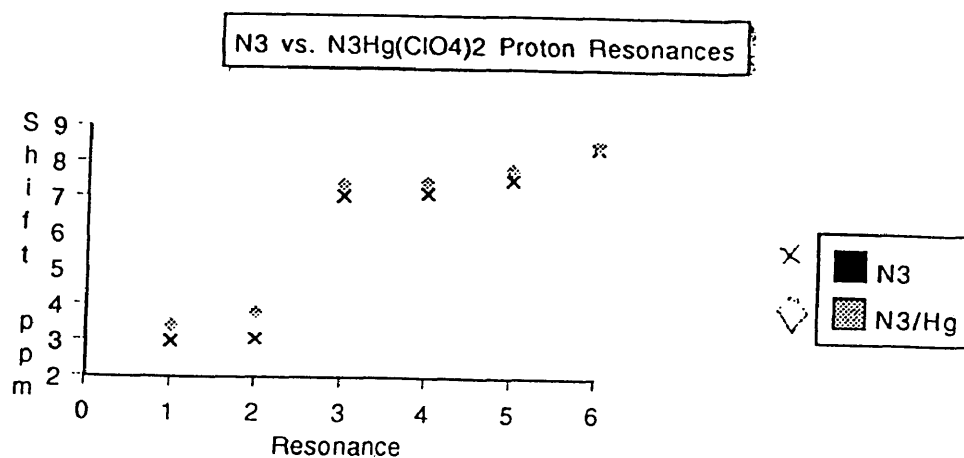
Figure 3.5 Proton NMR Resonances for N3 vs. an N3, N3/Hg Mix

The six peaks which have shifted downfield represent an average of the resonances for bound and unbound ligand. Some of the ligand is coordinated to mercury while some exists as unbound molecules. Later studies by Caryn Prairie showed even further downfield shift. We see an average of the peaks because ligand/ligand exchange is occurring more rapidly than the NMR timescale. The ^{13}C data supports this idea. There are seven peaks in the carbon spectrum which are slightly shifted from the seven peaks seen in the N3 carbon spectrum.

Table 3.6 Carbon 13 Resonances for
N3 vs. N3•Hg•(ClO4)2

N3•Hg•(ClO4)2 Resonances	N3 Resonances	Δ ppm
37.96	38.45	(0.49)
49.37	49.25	0.12
126.52	121.12	5.40
129.11	123.22	5.89
144.20	136.28	7.92
151.44	149.26	2.18
160.30	160.21	0.09
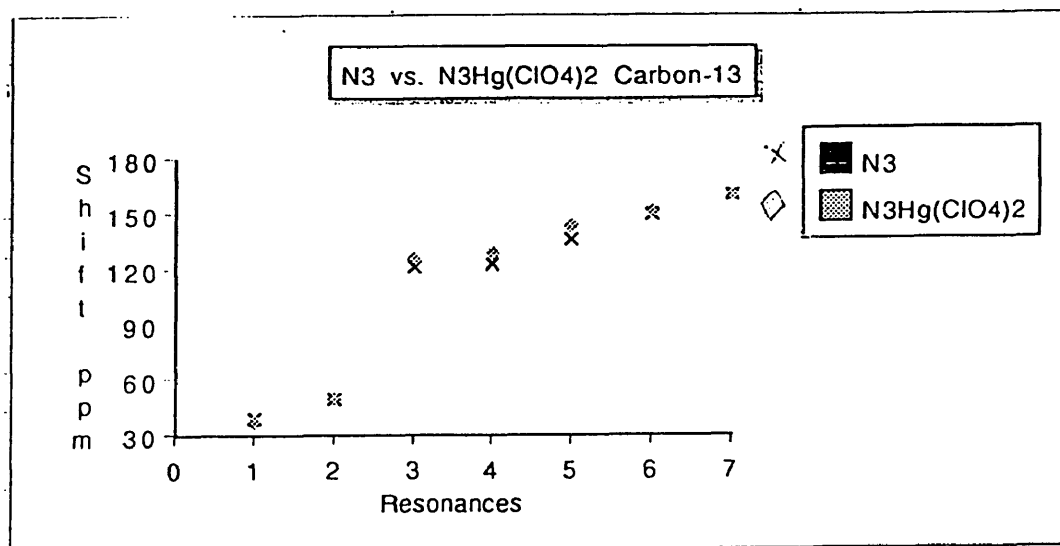
Figure 3.6 Carbon-13 Resonances for N3 vs. an N3, N3/Hg Mix

Since this complex had not been previously reported, there were no results to use

as a comparison. Variable temperature NMR experiments were performed on this

complex and are discussed later.

The ratio of reactants in the original synthesis was 3 to 1, ligand to mercury. The resonances in the proton NMR spectra shifted downfield, indicating coordination to mercury. It was then necessary to determine whether additional ligand would drive the equilibrium of the coordination to the right, causing more ligand to become bound; or whether that equilibrium had stabilized and additional ligand would only shift the average resonances upfield--in favor of unbound ligand. To answer this question, 3.96 mg of the crystals synthesized in Reaction (3.1) were dissolved in deuteracetone. Then, 1.1 mg (4.8 micromols) of ligand were added to the solution its proton NMR was acquired. The spectrum along with the spectrum for the crystals synthesized in 3.1 appear on page 66.

Addition of excess ligand caused the peaks to shift upfield, indicating that it shifted the equilibrium in Reaction (3.1) to the left-favoring unbound ligand. The ^{1}H spectrum is summarized below in Table 3.7.

Table 3.7 Proton Resonances (ppm) for N3•Hg•(ClO$_4$)$_2$ vs.
N3•Hg•(ClO$_4$)$_2$ + N3 vs. N3

N3•Hg•(ClO$_4$)$_2$	N3•Hg•(ClO$_4$)$_2$ + N3	N3
3.43	3.29	2.99
3.81	3.60	3.08
7.41	7.32	7.10
7.49	7.38	7.14
7.88	7.79	7.56
8.57	8.51	8.48

As is evident from Table 3.7, all resonances have shifted toward the right, nearer to the resonances for unbound ligand.

B. N3x•Hg(II)•I₂ [X=1-3]

In this synthesis (Reaction 3.2), N3 was coordinated to Hg (II) using iodide as a counterion. The room temperature proton spectrum for N3•Hg•I₂, located on page 65, is summarized in Table 3.8 and Figure 3.7 below.

$$3\ N3\ +\ HgI_2\ +\ HI\ \text{(aq)} \rightarrow\ N3x\text{•}Hg\text{•}I_2\ [X=1\text{-}3] \qquad (3.2)$$
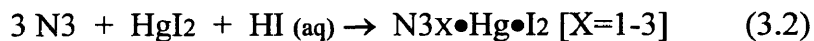
Table 3.8 Proton Spectra of N3•Hg•I₂ vs. N3

N 3•Hg•I₂ p p m	N3 ppm	Δ ppm (N3Hg-N3)
3.34	2.99	0.35
3.57	3.08	0.49
7.50	7.10	0.40
7.53	7.14	0.39
7.99	7.56	0.43
8.53	8.48	0.05
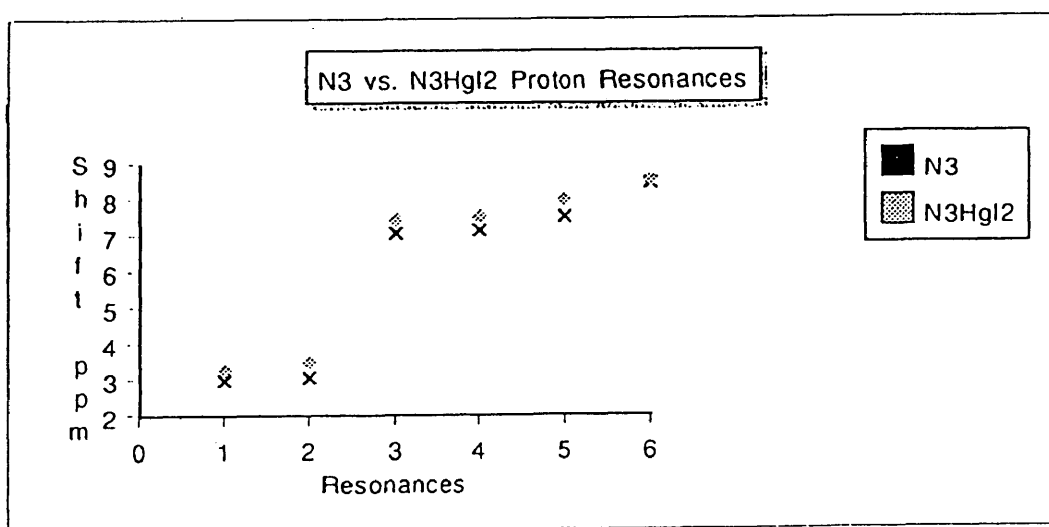
Figure 3.7 Proton Resonances for N3 vs. an N3, N3/Hg Mix

Carbon-13 data, located on page 65, is summarized in Table 3.9 and Figure 3.8.

Table 3.9 Carbon 13 Resonances for N3 vs. N3•Hg•I2

N 3•Hg•I2 Resonances	N3 Resonances	Δ ppm
31.88	38.45	-6.57
47.71	49.25	-1.54
124.24	121.12	3.12
125.59	123.22	2.37
140.34	136.28	4.06
149.13	149.26	-0.13
158.63	160.21	-1.58
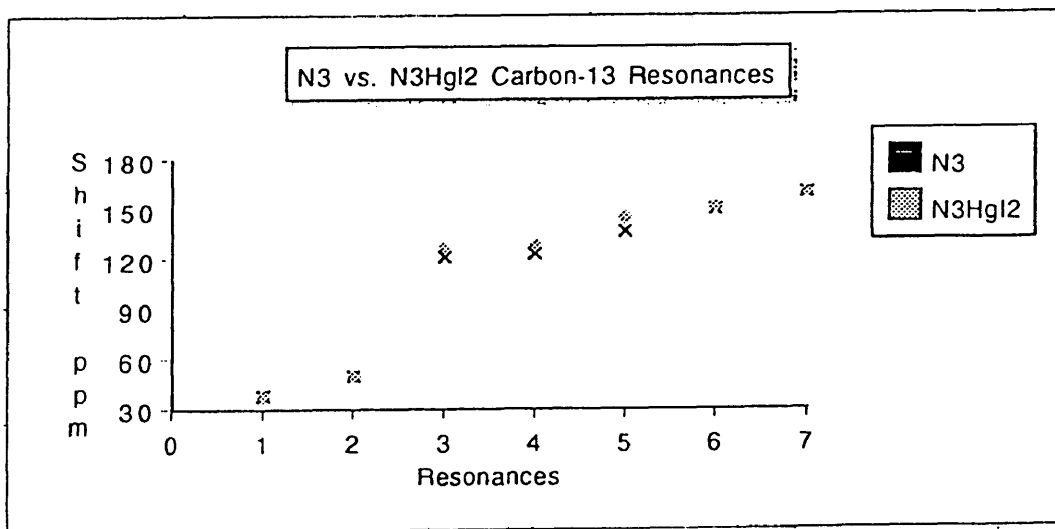
Figure 3.8 Carbon-13 Resonances of N3 vs. an N3, N3/Hg Mix

38

C. N3•Hg•(BF₃)₂

No crystals precipitated in this reaction. It was speculated that the crystals were highly soluble in water. In future reactions, use of a less polar solvent may facilitate precipitation.

III. METAL LIGATION DISCUSSION

In these coordination reactions, the degree of shift in the proton spectra was used as a general guide to estimate the extent to which ligand was bound to Hg(II). Because of exchange of ligand and the fact that no x-ray crystal structure was obtained, it was not possible to determine the exact composition of the crystals. A large shift in the proton spectrum was interpreted to mean that a greater proportion of the ligand was bound to Hg (II). This is because the observed signal is limited by the NMR time scale. A weighted average of the resonances is observed for bound and unbound ligand when a rapid exchange process is taking place. The more bound ligand is present, the further the resonances will be shifted away from those of unbound ligand.

Addition of excess ligand caused the peaks to shift to the right, back toward the resonances for pure ligand. This shows that when ligand is added to a complex synthesized with a 3 to 1 ratio of ligand to mercury the population of unbound ligand is increased. Ligand in excess of a 3 to 1 ratio of ligand to mercury does not increase the stability or population of bound mercury complexes. Instead, it increases the percent of unbound ligand present.

The other factor of interest was determining which counterion favored complex formation. By using the same ratio of ligand to mercury in both the synthesis with perchlorate and iodide, the larger downfield shift of the complex having perchlorate counterion suggested that perchlorate was a less coordinating counterion. The resonances for the crystals synthesized in Reaction (3.1) were shifted further to the left than the resonances for the crystals synthesized in Reaction (3.2). This evidence is consistent with the idea that there is a higher percentage of bound ligand present in the solution of crystals synthesized by Reaction (3.1), therefore having resonance averages closer to those of solely bound ligand. This result should be verified with samples constructed in NMR tubes from acetone solutions of ligand and metal salts to remove the composition ambiguity associated with isolation of crystals.

Because there were not two distinct sets of peaks for any of the complexes, we know that ligand/ligand exchange occurs more rapidly than the NMR time scale for detection of distinct sets of resonances. Low temperature spectra were taken in an attempt to slow ligand exchange to the point where distinct sets of resonances could be captured on an NMR timescale.

IV. VARIABLE TEMPERATURE NMR STUDIES

The Hg (II) complexes synthesized in this research were subject to rapid ligand/ligand exchange due to the low kinetic barrier between bound and unbound ligand. In enzymes the metal ligands are rigidly fixed in a single orientation. Furthermore, metal

ions tend to reside in clefts that are inaccessible to a second protein molecule as a catalyst for exchange processes. Hence, metals are somewhat less likely to become unbound because the metal cannot coordinate to the active site of two protein molecules at once.

By dissolving the crystals in deuterated acetone and performing variable low temperature spectroscopy, it was possible to cool the sample to -90°C. Lower temperatures have the potential to remove enough kinetic energy to slow ligand/ligand exchange to a rate where it is possible to characterize a stable ligand/Hg complex.

A. N3x•Hg (II)•(ClO4)2   [X=1-3]

Variable low temperature NMR was performed on the crystals synthesized in Reaction 3.1. They were dissolved in deuterated acetone and placed in an -90 °C liquid Nitrogen/Acetone bath prior to study to ensure that the crystals did not precipitate at lower temperatures. The spectra are located on pages 64 and 67 through 74. The data contained is summarized below in Table 3.10.

Table 3.10 Variable Temperature NMR for
N3•Hg•(ClO4)2

Temperature °C	Resonances							
	1	2	3	4	5	6	7	Page
20.0	3.43		3.81	7.41	7.49	7.88	8.57	64
0.00	3.42		3.80	7.41	7.48	7.89	8.58	67
-20.0	3.42		3.79	7.42	7.48	7.89	8.59	68
-40.0	3.41		3.78	7.45	7.48	7.89	8.60	69
-50.0	3.40	3.47	3.77	7.45	7.48	7.89	8.61	70
-60.0	3.40	3.57	3.77	7.45	7.48	7.89	8.63	71
-70.0	3.39	3.65	3.76	7.45	7.48	7.90	8.65	72
-80.0	3.39		3.74	7.45	7.48	7.90	8.66	73
-90.0	3.38	3.76	3.82	7.45	7.48	7.90	8.68	74
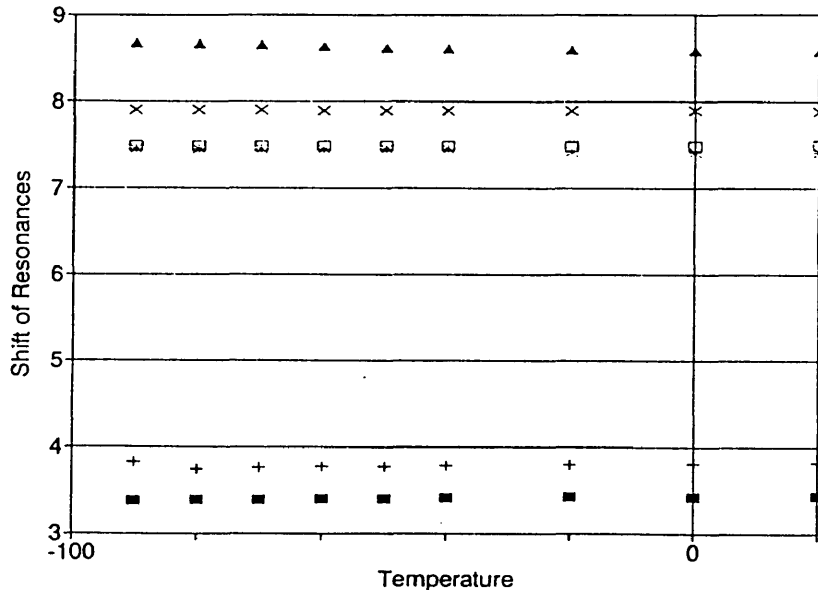
Figure 3.9 Variable Temperature NMR of
N3x•Hg (II)•(ClO4)2   [X=1-3]

It is obvious from the above data, that while Resonance 1 drifted slightly to the

upfield and Resonance 7 drifted slightly to the downfield, the other 4 resonances

remained roughly the same. A new peak emerged at lower temperatures and was

designated as Resonance 2. It shifted downfield as the sample cooled. This peak which

shifted between the two alkyl resonances during the study of N3•Hg•(ClO4)2 was most

likely the caused by the exchange labile hydrogen attached to the amine nitrogen of N3.

It is not surprising that this peak would both resonate in this region and exhibit a more

severe temperature dependence.

Ideally, we would have seen separate sets of resonances for unbound ligand and ligand

mercury complex. The slight drifting of peaks at lower temperatures is most likely due to a

temperature dependence of the resonances rather than separation of the separate sets of peaks.

The solution of crystals with excess ligand (see Chapter 3 Section II A) dissolved in

deuterated acetone was studied at -90 °C (p. 79). Because the resonances experienced an upfield

shift (favoring unbound ligand) upon addition of excess ligand, it was not expected that separate

sets of resonances would be seen at lower temperatures. The data collected, summarized below

in Table 3.11, confirmed this suspicion.

Table 3.11 Variable Low Temperature NMR Study of
N3•Hg•(ClO4)2 + N3

Temperature °C	Resonances							Page
	1	2	3	4	5	6		
20.0	3.29	3.60	7.32	7.38	7.79	8.51		66
0.00	3.33	3.70		7.42	7.86	8.66		67

Except for two of the aromatic peaks merging and a slight drifting of the resonances,

nothing noteworthy occurred at lower temperatures, as was anticipated.

B. N3X•Hg•I2 [X=1-3]

The N3X•Hg•I2 [X=1-3] crystals synthesized in Reaction (3.2) were also studied by

variable low temperature NMR experiments. The room temperature values reported earlier were

for crystals dissolved in acetonitrile. In order to take a wider range of spectra for these crystals,

they were dissolved in deuteracetone and placed in an NMR tube. The tube was immersed in a -

90 °C liquid Nitrogen/Acetone bath to ensure that compound would not precipitate at lower

temperatures. The low temperature spectra appear on pages 75 through 78 and are summarized

below in Table 3.12. Figure 3.10 is a graphical representation of this data.

Table 3.12 Variable Low Temperature NMR for
N3X•Hg•I2   [X=1-3]

Temperature °C	Resonances							Page
	1	**2**	**3**	**4**	**5**	**6**		**Page**
0.0	3.49	3.88	7.46	7.56	7.95	8.61		75
-40.0	3.48	3.86	7.47	7.56	7.96	8.64		76
-50.0	3.47	3.85	7.48	7.57	7.97	8.65		77
-70.0	3.46	3.84	7.48	7.57	7.97	8.68		78
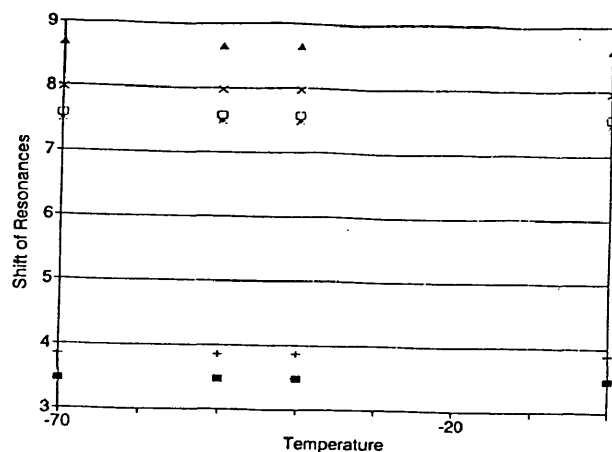
Figure 3.10 Variable Low Temperature NMR for
N3X•Hg•I2   [X=1-3]

Except for some slight drifting of resonance peaks, nothing noteworthy occurred at lower

temperatures. Ideally, we would have seen separate sets of resonances for unbound ligand and

ligand mercury complex. The slight drifting of peaks at lower temperatures is most likely due to

a temperature dependence of the resonances rather than separation of the separate sets of peaks.

4

Conclusion

What we are ultimately interested in is recording the resonances for Hg bound

ligands. It is thought that the ligands discussed previously-N3, N4, and N3S- along

with other variations on the same basic design mimic enzyme active sites containing

histidine, cysteine, and methionine. The implications of this structural analogy is that

ligand resonances when bound to Hg (II) should very closely approximate those of

enzyme amino acid residues bound to Hg (II).

It has been shown in this research that the proton resonances of the dihistidine-

like compound, N3, experience a leftward shift when bound to mercury. Established

NMR Theory, discussed in Appendix A) suggests that this is caused by the mercury ion

drawing

electron density away from the N3 protons. Because Hg(II) has a positive charge, it is not surprising that it draws electron density away form molecules coordinated to it.

Ideally, even at room temperature, two distinct sets of peaks would appear--one for ligand and one for ligand/Hg complex. What we have seen thus far is an average of the resonances for N3 and mercury bound N3. However, we have also determined that ligand in excess of a 3 to 1 ligand to mercury ratio increases the percent of unbound ligand present. This increased amount of unbound ligand causes the observed peaks to shift toward those of pure ligand.

Also discovered in this research is that Perchlorate ions allow for a greater shift in resonance than Iodide ions do. This is most likely the result of enhanced stability of the ligand/mercury complex which would slow down some of the ligand-ligand exchange, perhaps increasing the amount of ligand/Hg complex in solution and weighting the average resonance in favor of this complex.

The direction in which to proceed is clearly to synthesize complexes with a smaller excess of ligand or with Hg(II) in excess. These compounds will hopefully display distinct sets of resonances which approximate the resonances of histidine binding sites in enzymes.

Once the optimum ligand to mercury ratio is established, synthesis of organometallic complexes containing ligands that are more difficult to manufacture

should be begun. N4 synthesis and purification procedures have been satisfactorily established. This would be the most obvious choice for the next molecule to coordinate.

Work begun on N3S is promising and methylation of the thiol group should bring us closer to purifying and positively identifying this ligand. Synthesis begun on the starting material for a propyl-bridged series analogous to the ethyl-bridged N3, N4, and N3S discussed in this text should be continued and perfected.

Though distinct resonances for mercury bound N3 were not found, the information gained during the course of the research has laid the foundation for future research on the same topic.

Appendix A

NMR Theory

Since the NMR instrument was a crucial research device, a brief overview of the theory behind its operation should be helpful.[1-3] The most often used experiment was proton spectroscopy followed by Carbon-13 NMR. As the research continues, ^{199}Hg and 2-D spectroscopic techniques may also be applied.

A. Proton Spectroscopy

Nuclear magnetic resonance spectroscopy (NMR) makes use of the magnetic properties of nuclei with half integer quantum spin number. Using this technology, we are able to gain information about the chemical structure of molecules.

As a proton spins, a magnetic field perpendicular to the spin axis of the nucleus is generated. This gives the nuclei magnetic moments which, under normal circumstances, are randomly dispersed.

In NMR Spectroscopy, a sample is placed above a powerful magnet which is used to align the magnetic moments of the nuclei. The moments can be aligned either with or against the applied magnetic field. Moments aligned with the field have a lower energy and thus a slightly higher population than moments aligned against the field.

The sample is pulsed with electromagnetic radiation and the nuclei absorb quantized amounts of energy. This energy is then emitted by the nuclei and received by a detector as the nuclei relax back to their original state. The energy emitted, known as a magnetic resonance, is collected by a detector as a group of cosine waves superimposed upon each other. These signals are separated by a complex mathematical process, known as Fourier Transformation, into a spectrum which gives information about the chemical environment of the individual nuclei.

Magnetic resonances are usually reported in units of parts per million (ppm) which correspond to the frequency (in hertz) of the energy they absorb. The chemical environment affects the exact frequency of resonance as will be discussed later. Tetramethyl silane (TMS) is often used as an internal standard to calibrate the instrument and its signal is assigned a resonance of 0.00 ppm. Peaks for resonances span the region to the left of this peak, from 0.00 to about 10.0 ppm for proton spectra. Peaks located to the left in the spectrum are said to be "downfield" and peaks located to the right are said to be "upfield". Nuclei which resonate downfield absorb energy of a lower frequency than those occurring further upfield.

The location or frequency of a resonance in the spectrum is determined by how "shielded" the proton is. The electrons circling a proton, including the ones shared in bonds, generate a magnetic field that in most cases opposes the electromagnetic radiation. For protons which are more "shielded" by the induced field, a higher frequency of electromagnetic energy is required for absorption. Therefore, they are found further upfield.

Since the magnitude of the shielding is a direct result of electron density surrounding the nucleus, there are two factors which have a large impact on the degree of shielding experienced by a nucleus. The bond type that the proton is involved in has a shielding affect as follows: $sp^2 < sp < sp^3$. This can be explained by the fact that sp^2 orbitals delocalize electron density so the induced field opposing the external field is weaker. sp orbitals delocalize electron density to a lesser extent therefore shielding more. Electrons in sp^3 orbitals almost always shield protons the most. There are exceptions to this rule.

The other factor affecting shielding is the electronegativity of neighboring atoms. Electronegative atoms draw electron density away from neighboring nuclei, causing them to become more deshielded and therefore causing them to resonate further downfield. This phenomenon becomes less effective over distances of more than three bond lengths.

Besides the chemical shift of nuclei, there is another useful property detectable by NMR--that of spin-spin coupling giving rise to signal splitting. The moments of the protons on neighboring nuclei are also aligned either against or with the field. This results in the signal of the resonating nuclei having a slightly higher or lower resonance, depending on its neighbor's alignment, than if it were isolated and so the signal is split.

In general, if a proton has n neighboring protons, its signal will be split into n-1 peaks. Splitting patterns can often give much useful information; but as molecules become more complex, peaks often overlap or patterns become too complicated to decipher.

B. ^{13}C and ^{199}Hg Spectroscopy

In addition to proton spectroscopy, there are two other 1-D NMR techniques that are and will be important to the research--^{13}C and ^{199}Hg NMR. These nuclei both have spin numbers of 1/2 and they can be studied with only slight variations on the technique used for ^{1}H NMR.

Though the most abundant isotope of carbon, ^{12}C, has a spin=1, making it useless for spectroscopic study, ^{13}C has a spin of 1/2. While its isotopic abundance is only 1.11 %, the signal to noise ratio can be improved by increasing the number of data points collected.

Because of the low relative abundance of the ^{13} C isotope, spin-spin coupling

between carbon atoms does not result in observable signal splitting. Attached hydrogen

atoms, however, due cause the signal to split, again with n attached hydrogens giving

rise to n+1 peaks. In order to obtain a spectrum which does not display this spin-spin

coupling between carbons and hydrogens, a proton decoupler can be used. This kind of

spectrum is referred to as a proton-decoupled spectrum.

^{13} C spectra give information about the number and kind of carbons present in

the carbon skeleton. Carbon atoms generally resonate in the range of 0 ppm- 200 ppm,

which often makes the spectra less complicated than those of proton spectra by

spreading the peaks over a wider area. For the most part, more highly deshielded

carbons, such as those found in aromatic rings, are located further downfield than those

which are more shielded.

^{199} Hg has a spin quantum number of 1/2 and can also be studied directly by

NMR. A special heteronuclear probe is required for studies of this type. This isotope

has a relative abundance of 16.84% [4] which makes spin-spin coupling more probable.

C. 2-Dimensional Spectroscopy

Advances in NMR technology have made it possible to obtain 2-Dimensional

Spectra which give us information about the connectivity of the nuclei being studied.

These experiments can be either homonuclear or heteronuclear. Table A.1 summarizes some of the available experiments and describes their usefulness.

Table A.1 Common 2-D NMR Experiments

Connectivity	Experiment	Application
^1H-^1H	Homonuclear COSY	Determines which H's are attached to adjacent carbons
^1H-^{13}C	Heteronuclear COSY	Determines which hydrogens are attached to which carbon nuclei
^{13}C-^{13}C	INADEQUATE	Determines which carbon nuclei are adjacent, low sensitivity
^1H-^1H	NOESY	Determines which hydrogens are in close 3-D proximity

While an in depth discussion of these techniques is not necessary for the ideas presented in this text, suffice it to say that these and other variations of these techniques are making complex problems easier to solve. 2-Dimensional spectroscopy should be extremely useful as this research develops.

Appendix B

Spectral Data and GC Traces

On the following pages you will find the NMR and GC/MS data referred to throughout this text. As previously stated, all NMR spectra were acquired on a QE-300 spectrometer run by the CHARM software program.

The gas chromatographic/mass spectral data was acquired on a Hewlett Packard 5890 gas chromatographer in conjunction with a mass spectrometer. This instrument was run using MS-Top Chem Station software. All relevant instrumental parameters were listed previously in the experimental sections.

With regards to the NMR spectra, the title and page number were added subsequent to printing the original research. All quantitative information deemed important was presented in the experimental section.

Bis-2-(2-pyridylethyl)amine

Top: ¹H NMR; Bottom: ¹³C NMR
Deuterated Chloroform
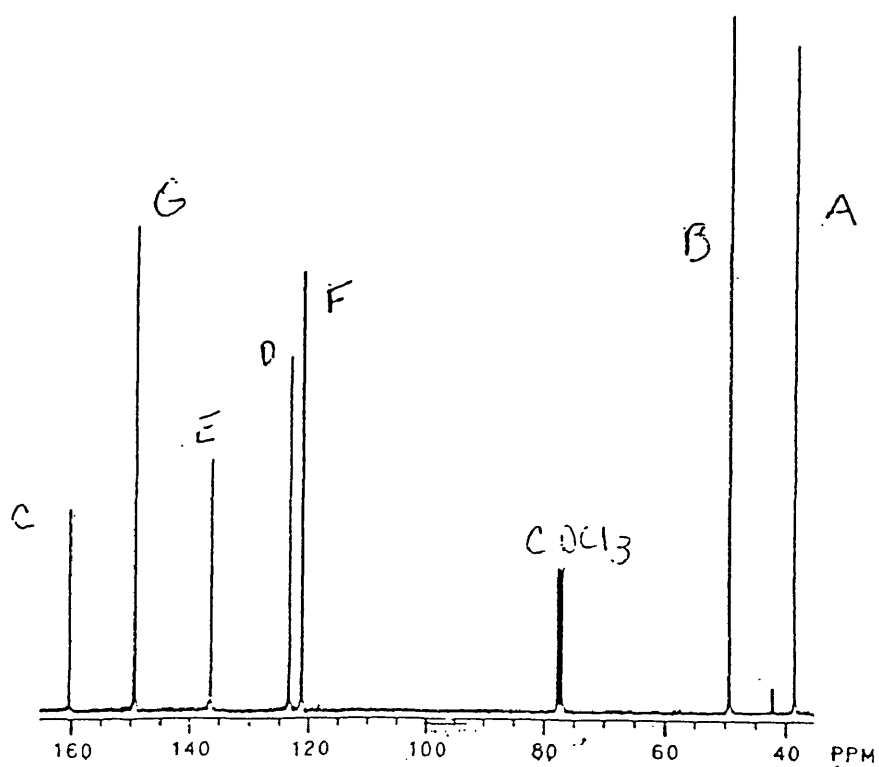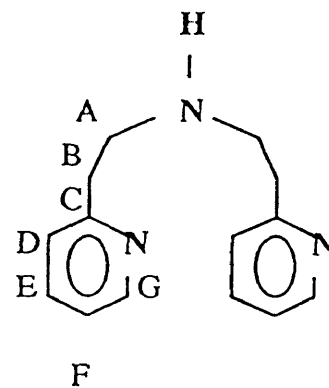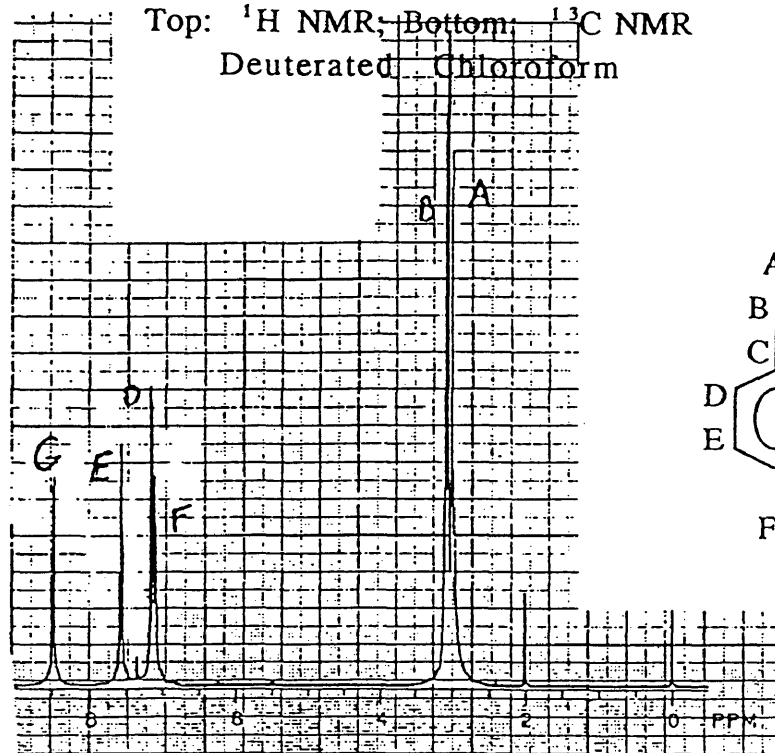
File: C:\CHEMPC\DATA\SRF17.D
Operator: SHARON
Date Acquired: 16 Aug 94   3:49 pm
Method File: DCB1.M
Sample Name: N38/2
Misc Info: Chloroform
ALS vial: 1

Abundance   TIC: SRF17.D

8.18

3000000

2500000

2000000

1500000

1000000

500000

0
Time ->   4.00   6.00   8.00 10.00 12.00 14.00 16.00 18.00

Abundance   Scan 433 (8.139 min): SRF17.D
                                    106   135
400000

350000

300000

250000

200000   93

150000   78

100000   65

50000   39 51   121

      25   149   170 183 195 210   227
0
M/Z ->   20   40   60   80   100   120   140   160   180   200   220
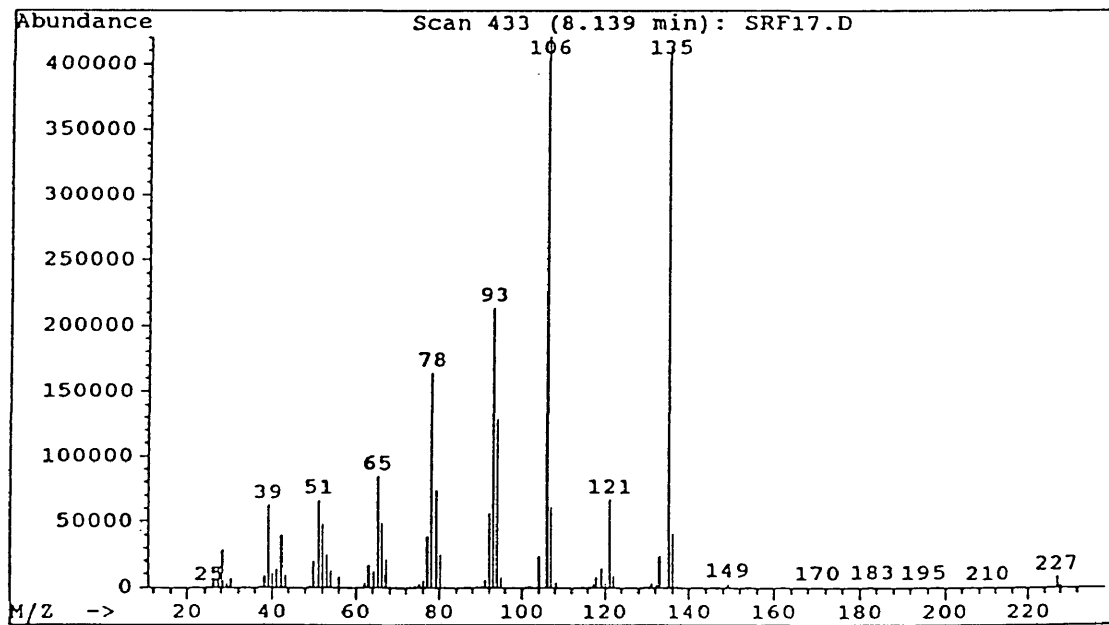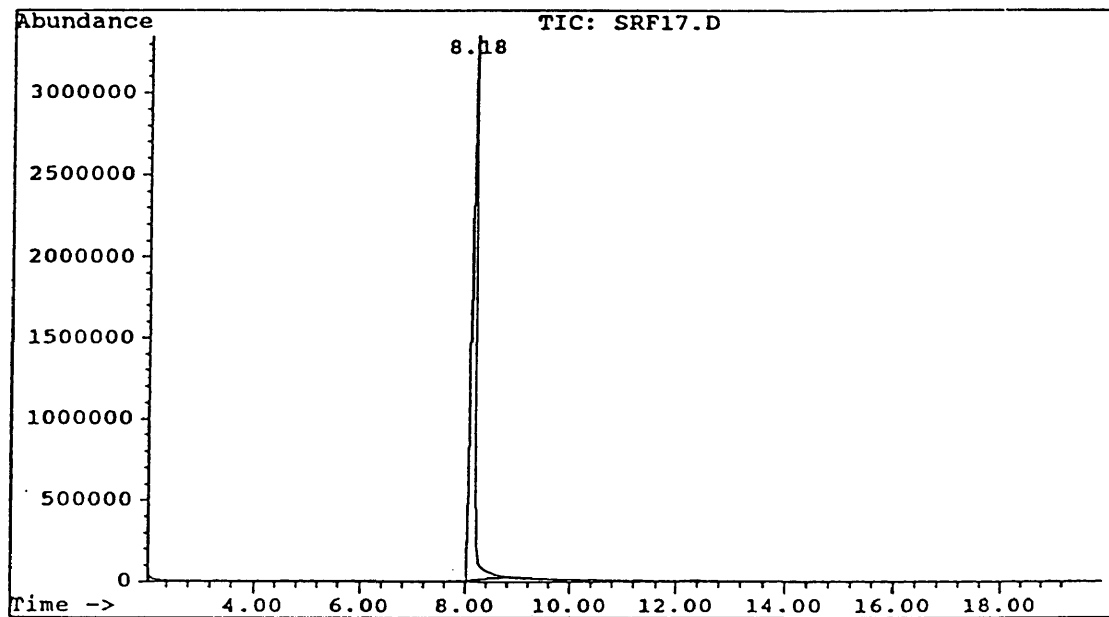
2-(3-Hydroxypropyl)pyridine
Top: ^1H NMR; Bottom: ^{13}C NMR
Deuterated Chloroform
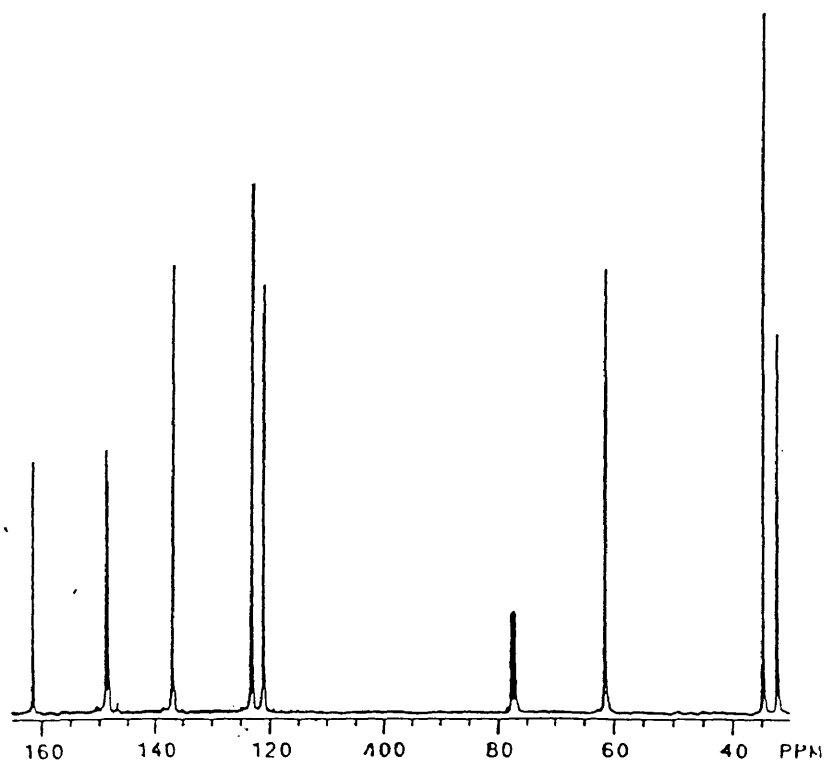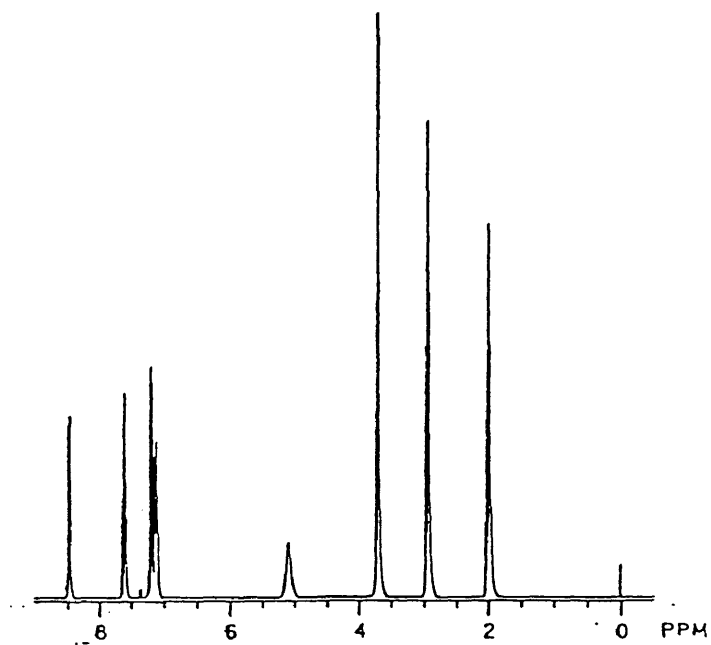
File: C:\CHEMPC\DATA\SRF014.D
Operator: Sharon
Date Acquired: 16 Sep 94   11:01 am
Method File: DCB2.M
Sample Name: 2-(3-Hydroxypropyl)pyridine starting material
Misc Info: Comparison with end product of bromination.
ALS vial: 1

TIC: SRF014.D

Average of 4.573 to 5.698 min.: SRF014.D (+,*)
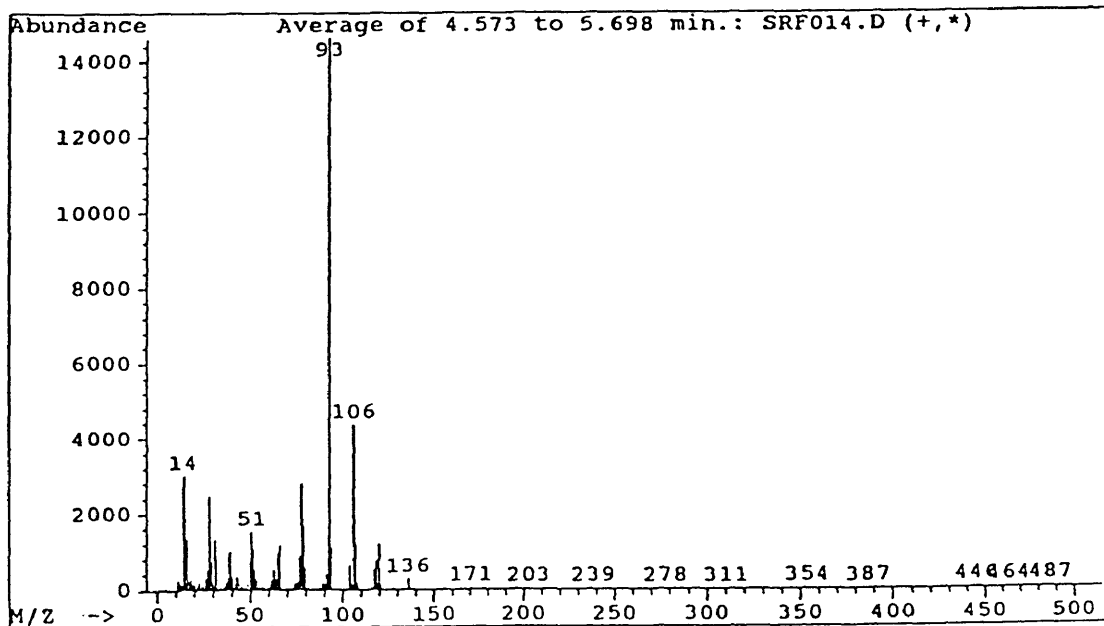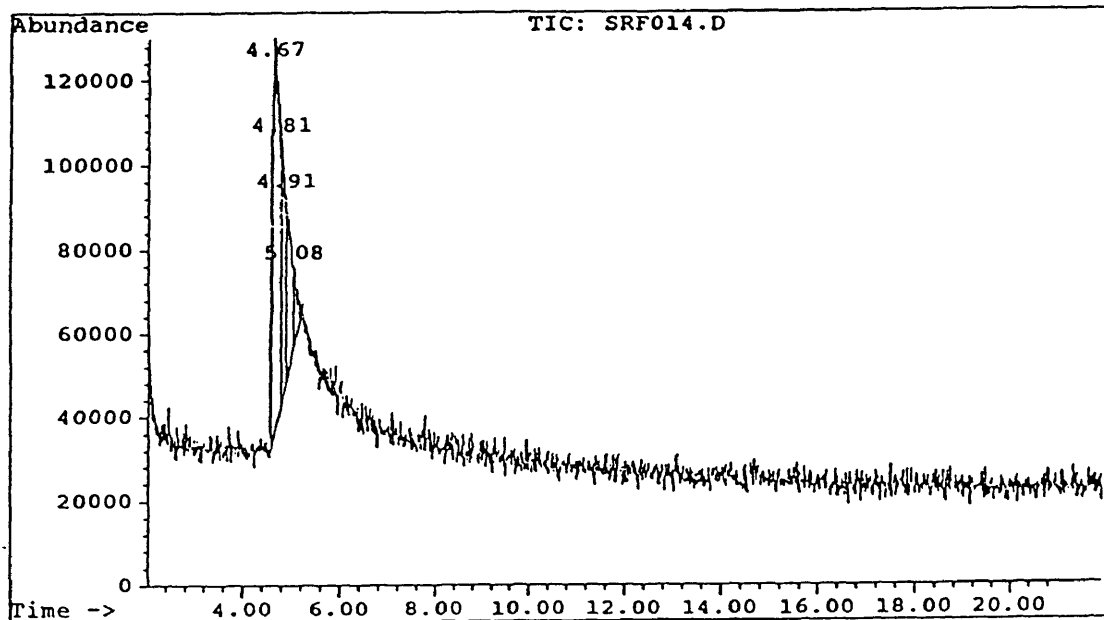
Tri-(2-(2-pyridylethyl)amine
Top: ¹H NMR; Bottom: ¹³C NMR
Deuterated Chloroform
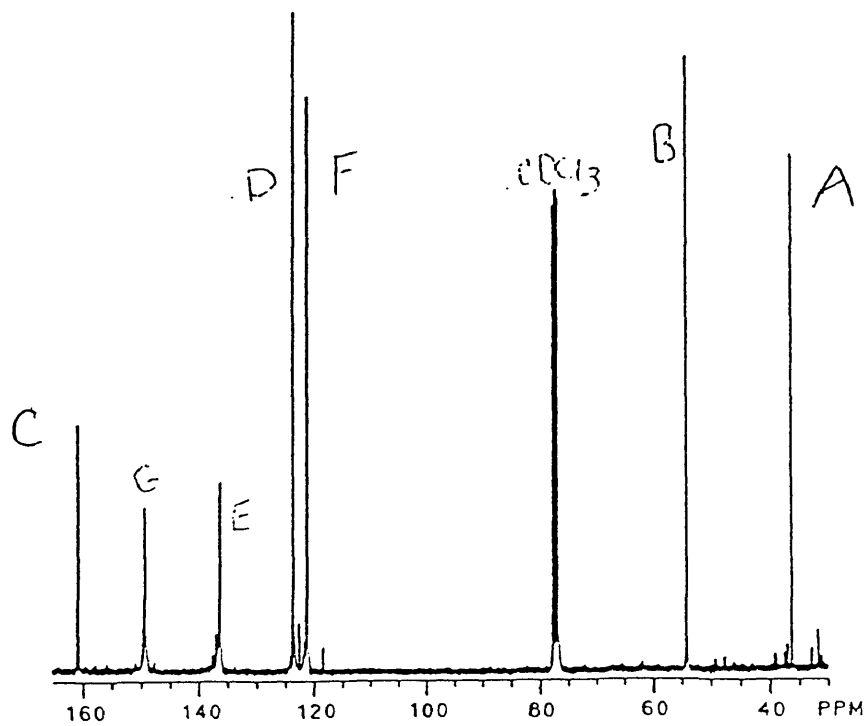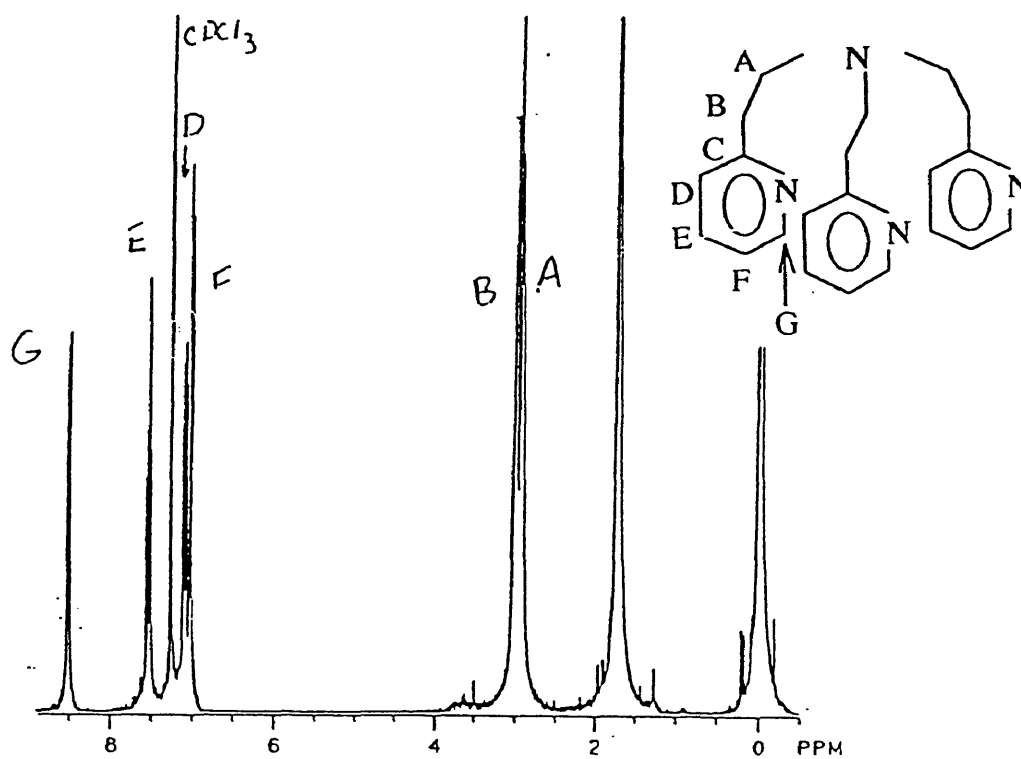
Tri-(2-(2-Pyridylethyl))amine

File: C:\CHEMPC\DATA\SRF2.D
Operator: SRF
Date Acquired: 31 Aug 94   9:05 am
Method File: DCB.M
Sample Name: N4RXN15FRAC13-24
Misc Info: TRIAL 3
ALS vial: 1
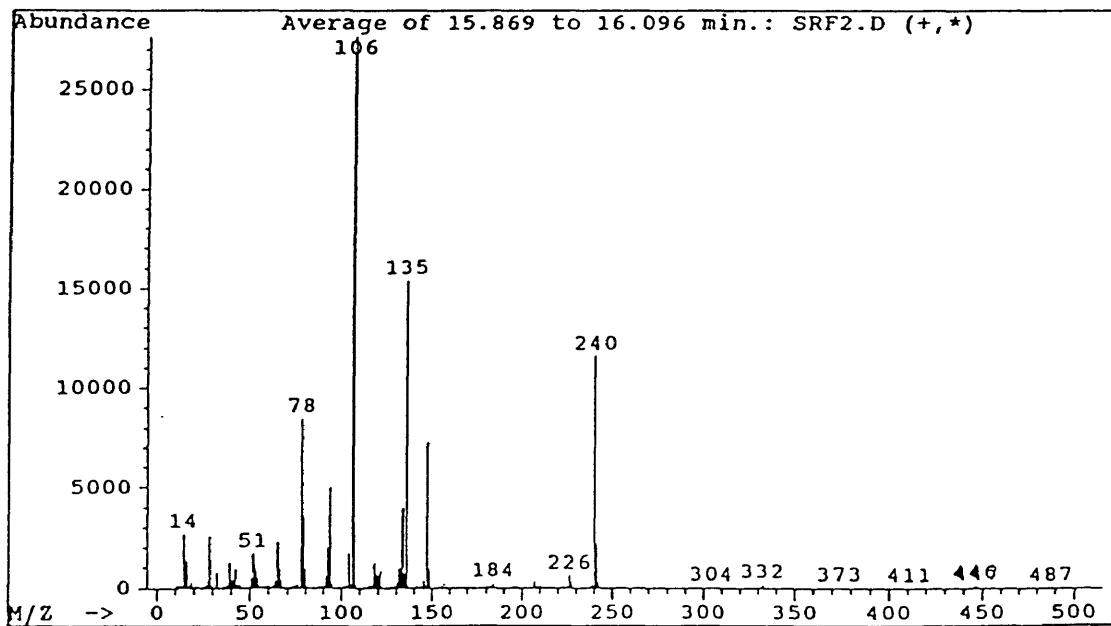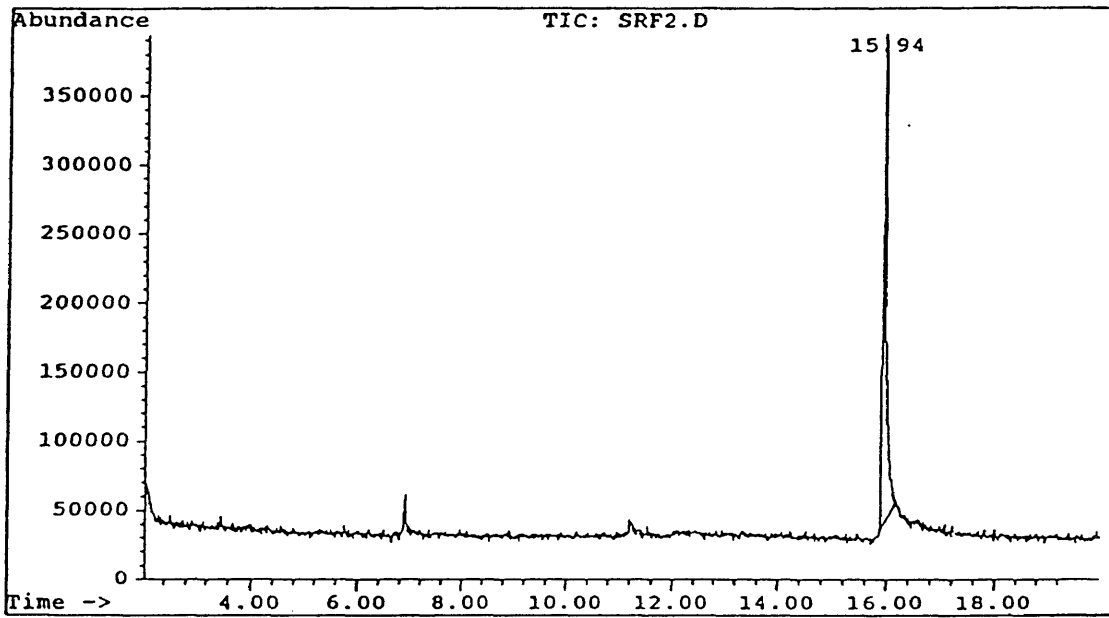
N3S Trial 2 Reaction Mixture
Top: ^{1}H NMR; Bottom: ^{13}C NMR
Deuterated Chloroform
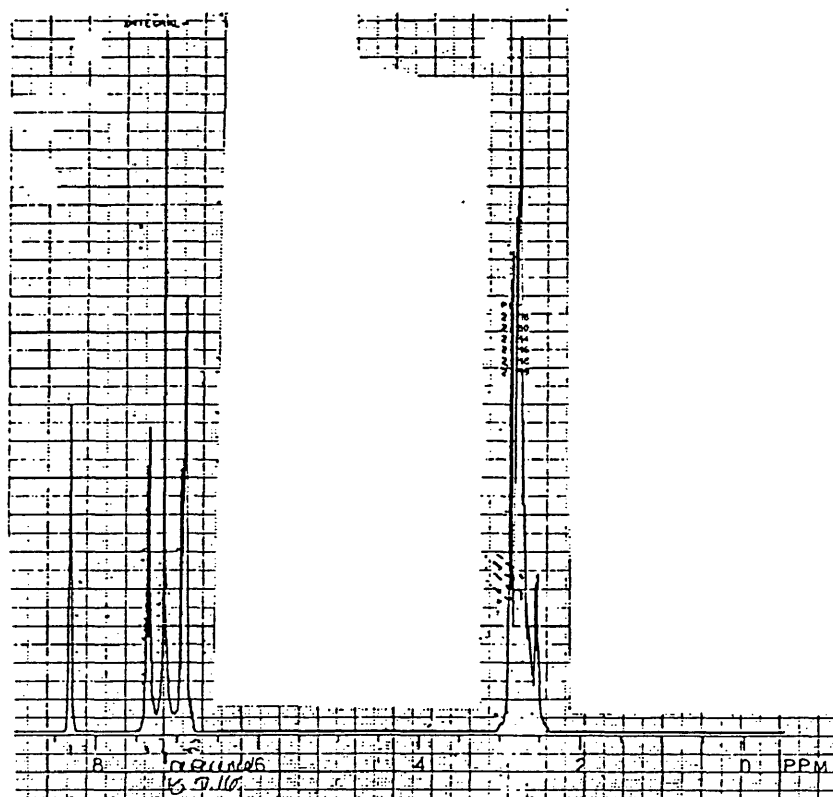
N3S Trial 2 Reaction Mix

File: C:\CHEMPC\DATA\DCB2.D
Operator: sharon
Date Acquired: 9 Jun 94   4:49 pm
Method File: DCB1.M
Sample Name: n3s
Misc Info:
ALS vial: 1

TIC: DCB2.D

Average of 11.483 to 13.292 min.: DCB2.D (+,*)
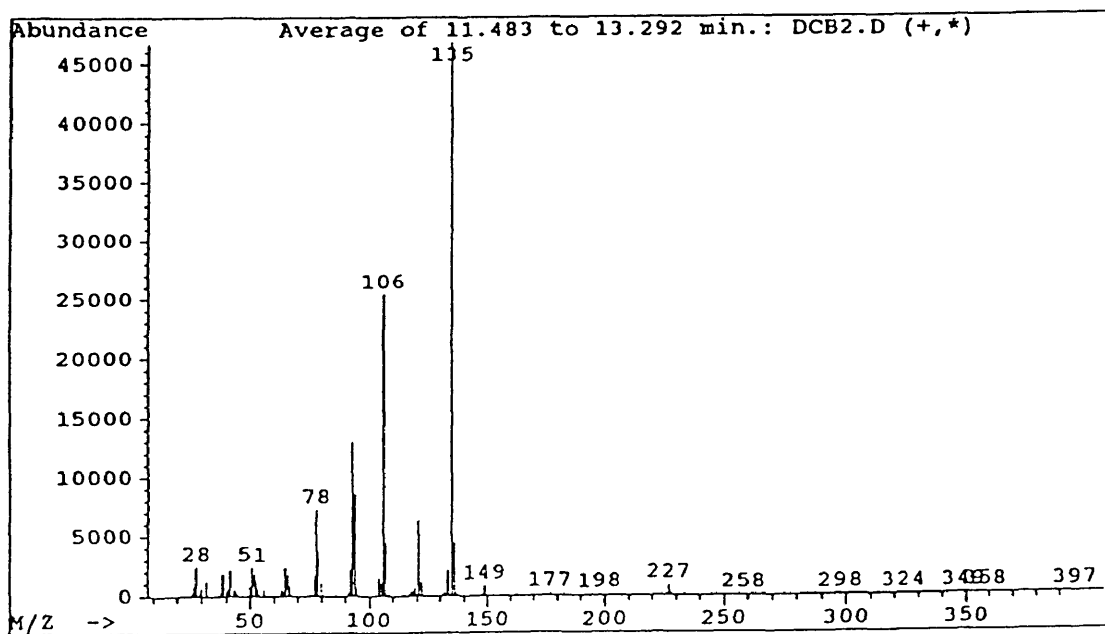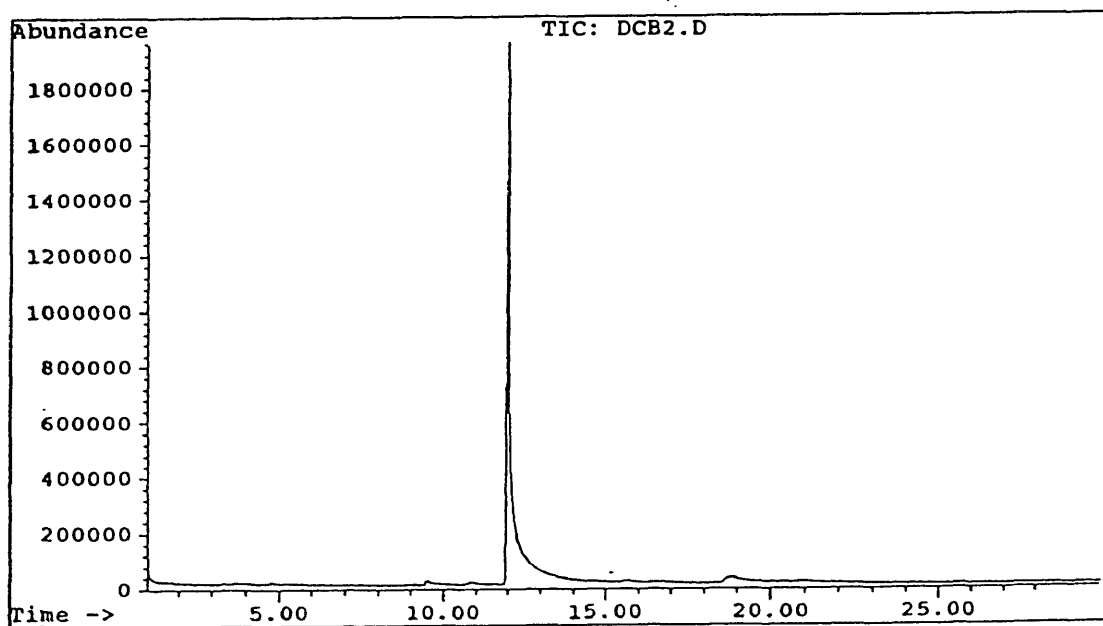
2-(3-Bromopropyl) pyridine
Trial 3 Reaction Mix
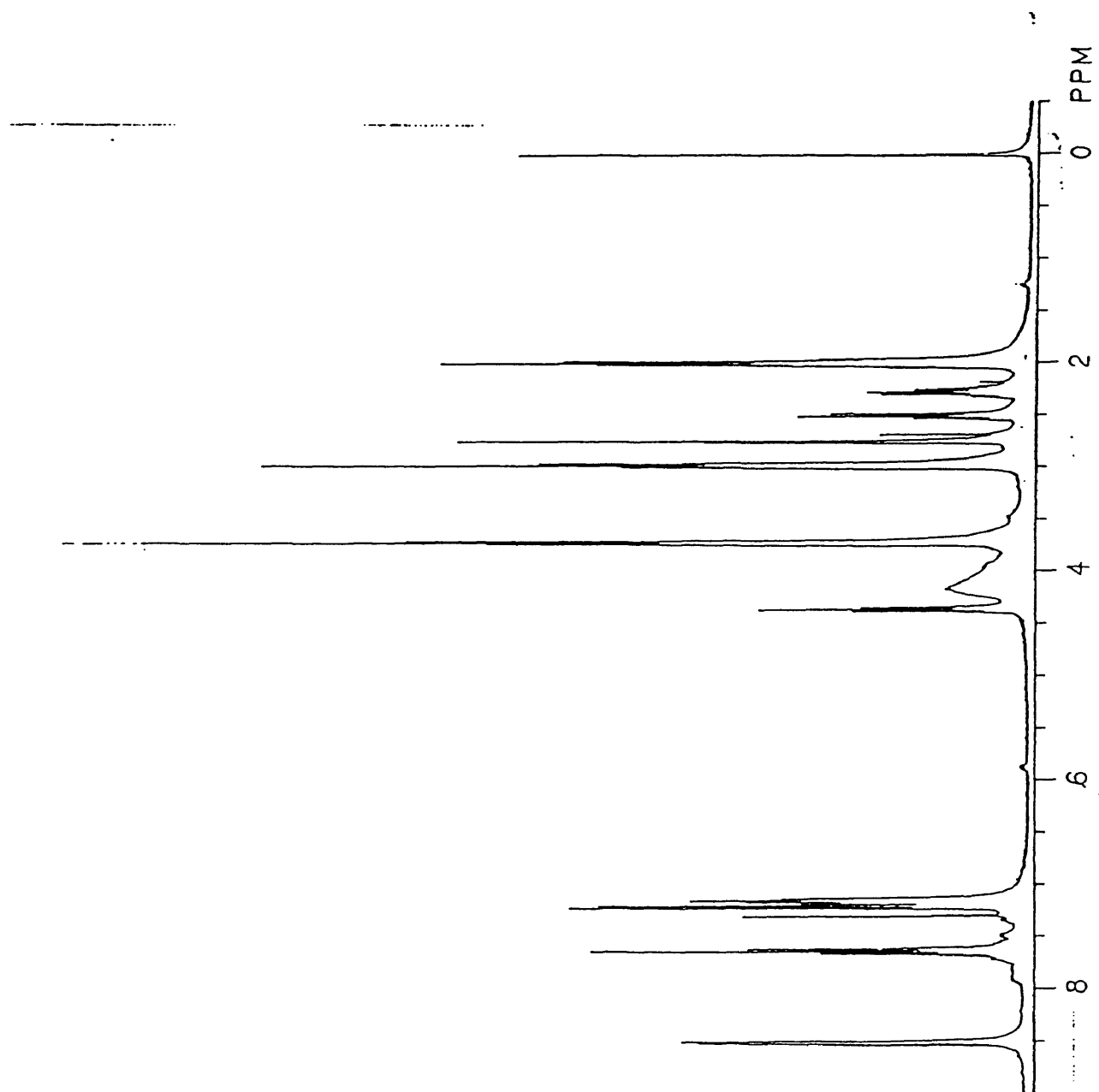
2-(3-Bromopropyl) pyridine
Trial 3 Reaction Mix

File: C:\CHEMPC\DATA\SHARON.D
Operator: Sharon Fitzhenry
Date Acquired: 22 Sep 94   2:37 pm
Method File: DCB2.M
Sample Name: 2-(3-Bromopropyl)pyridine
Misc Info: Third Attempt, Recrystallized NBS
ALS vial: 1
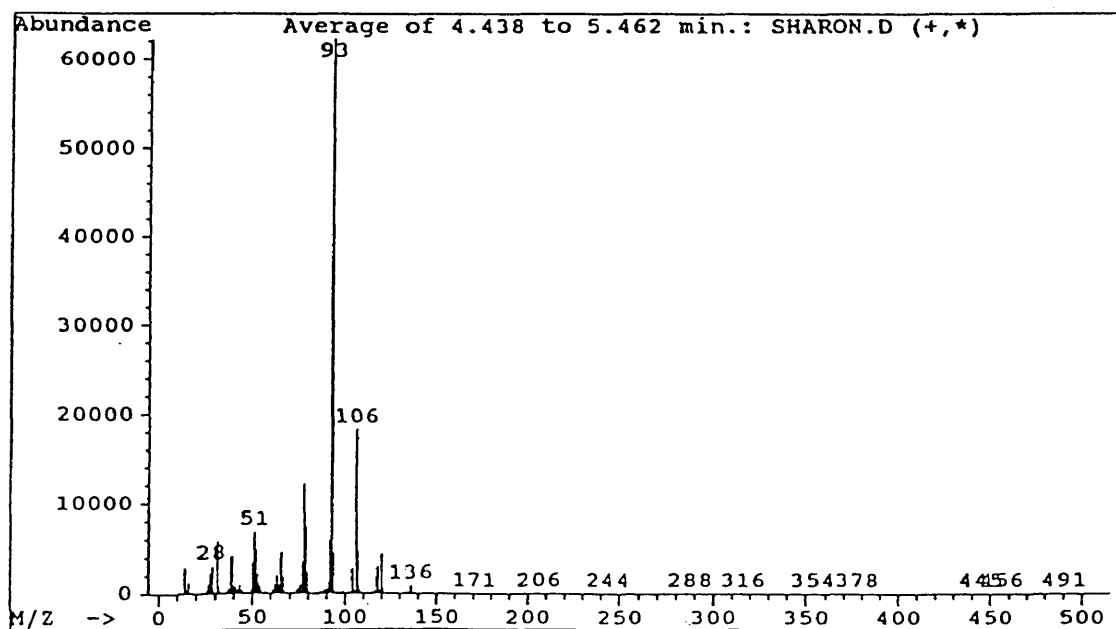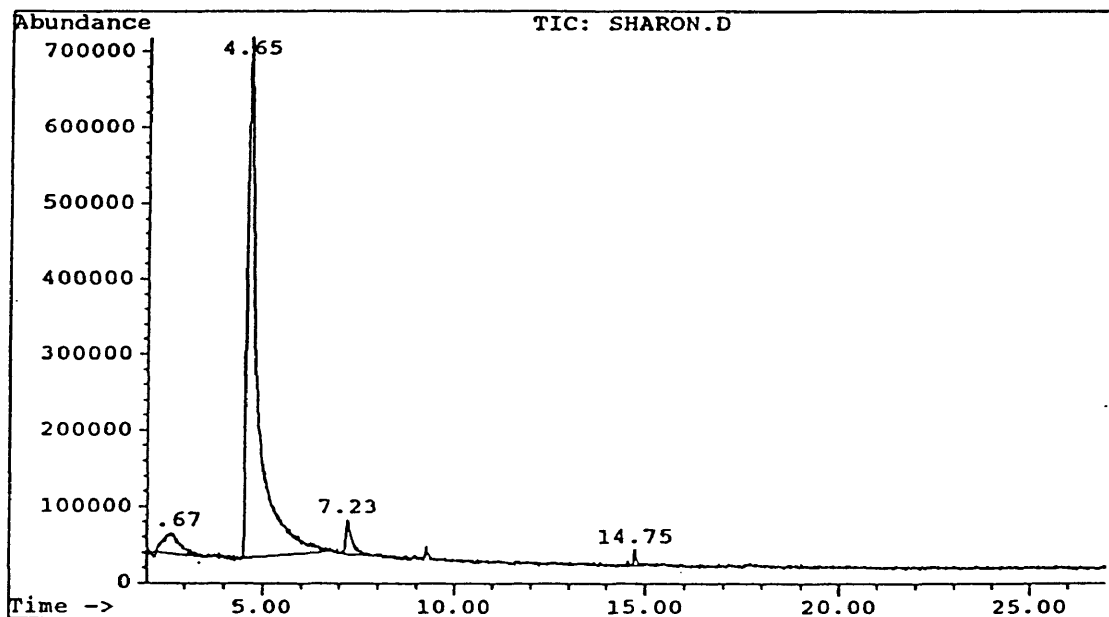
N 3$_x$•Hg (II)•(ClO$_4$)$_2$ [x=1-3]
Top: ^{1}H NMR; Bottom: ^{13}C NMR
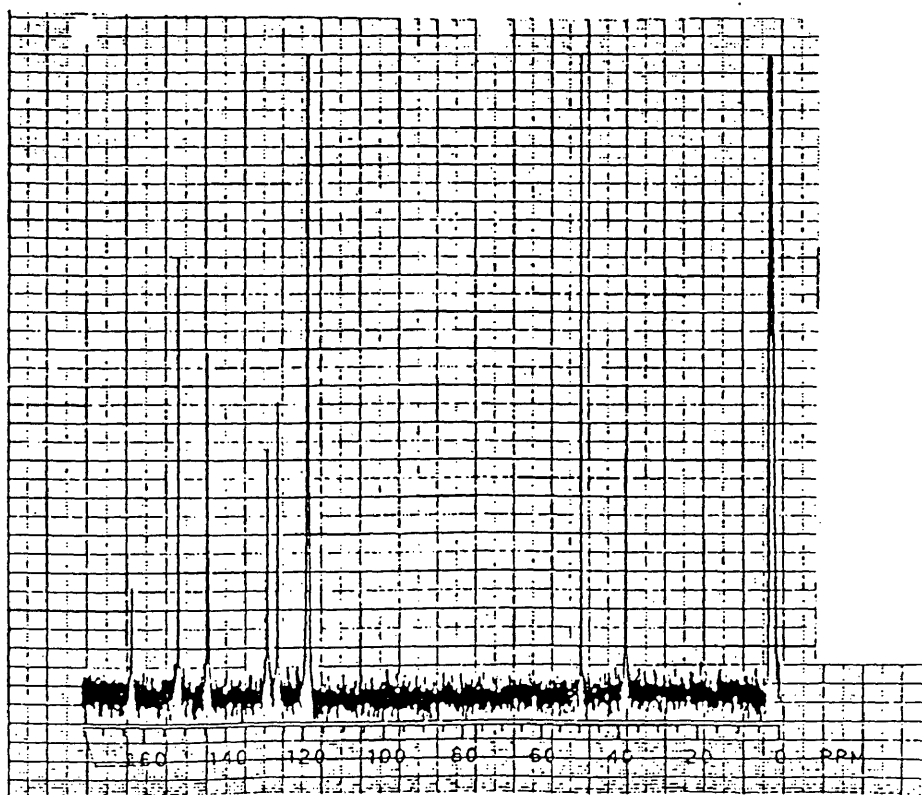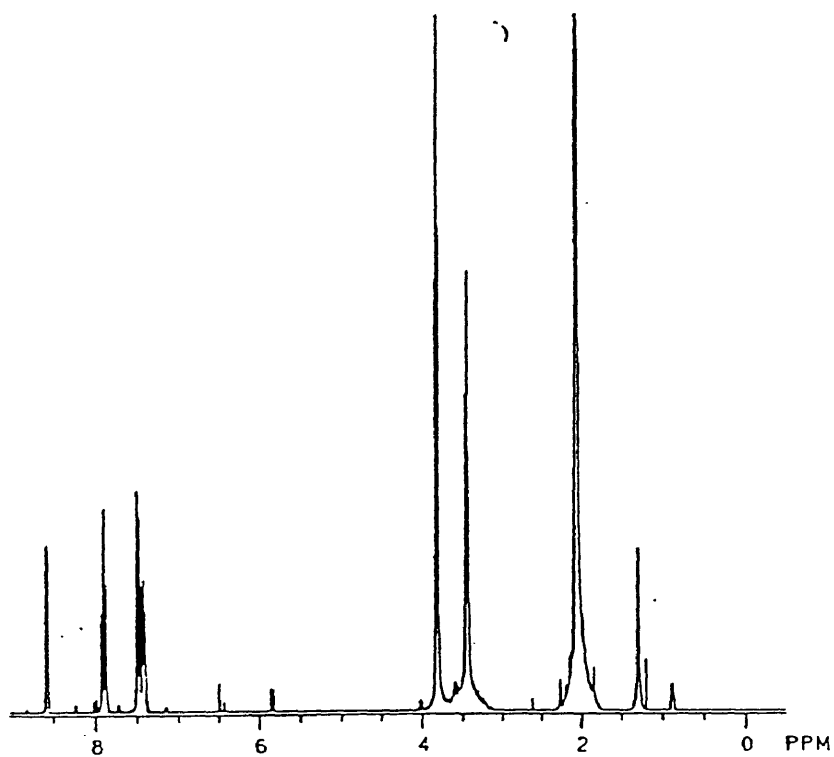
N 3ₓ•Hg (II)•I₂ [x=1-3]
Top: ¹H NMR; Bottom: ¹³C NMR
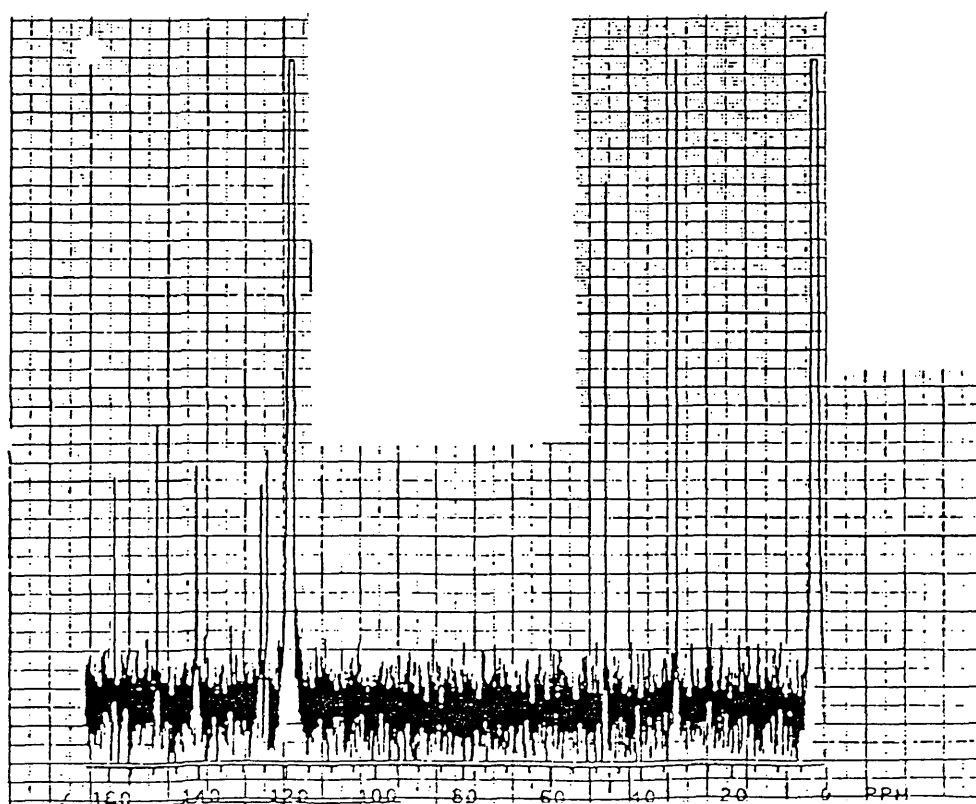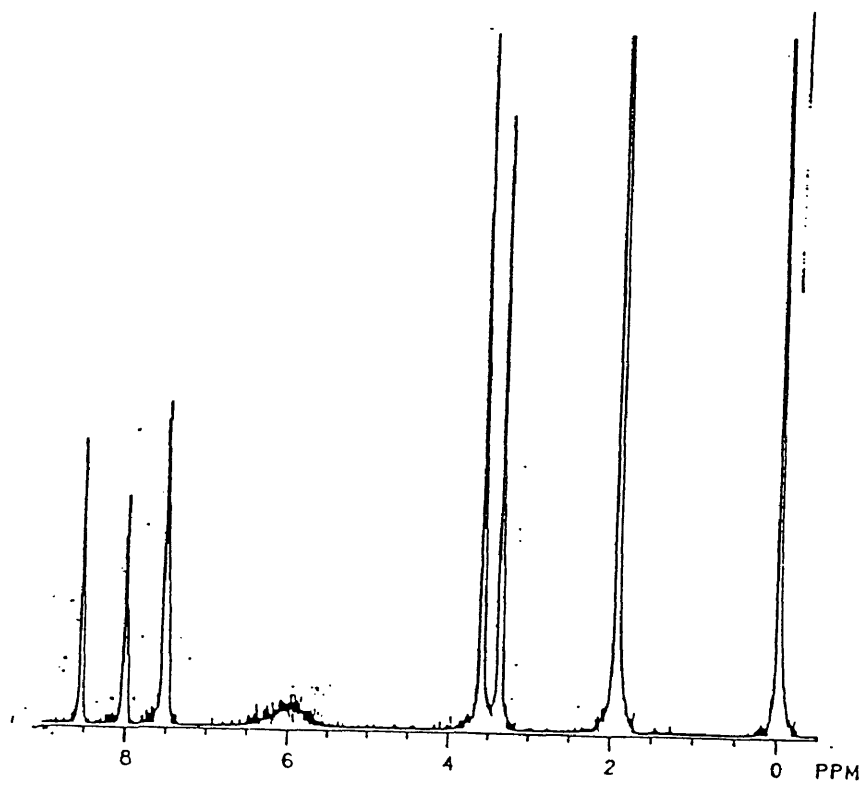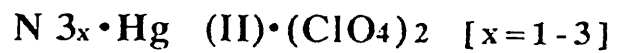
N 3$_x$•Hg (II)•(ClO$_4$)$_2$ [x=1-3]
Top: ^{1}H NMR Original Experiment
Bottom: ^{1}H NMR Same with additional N3
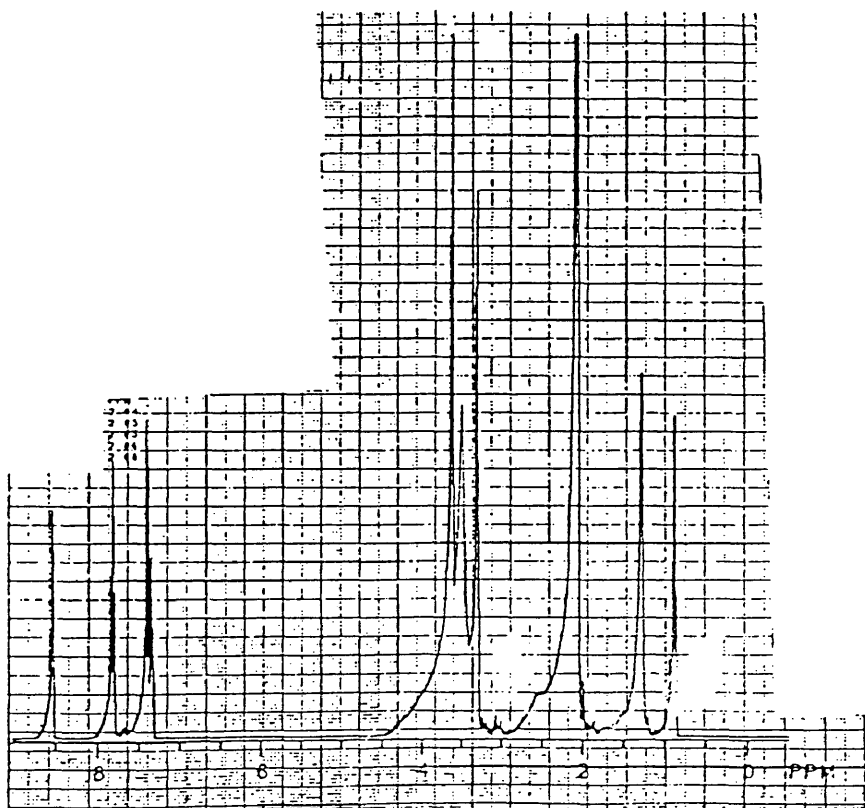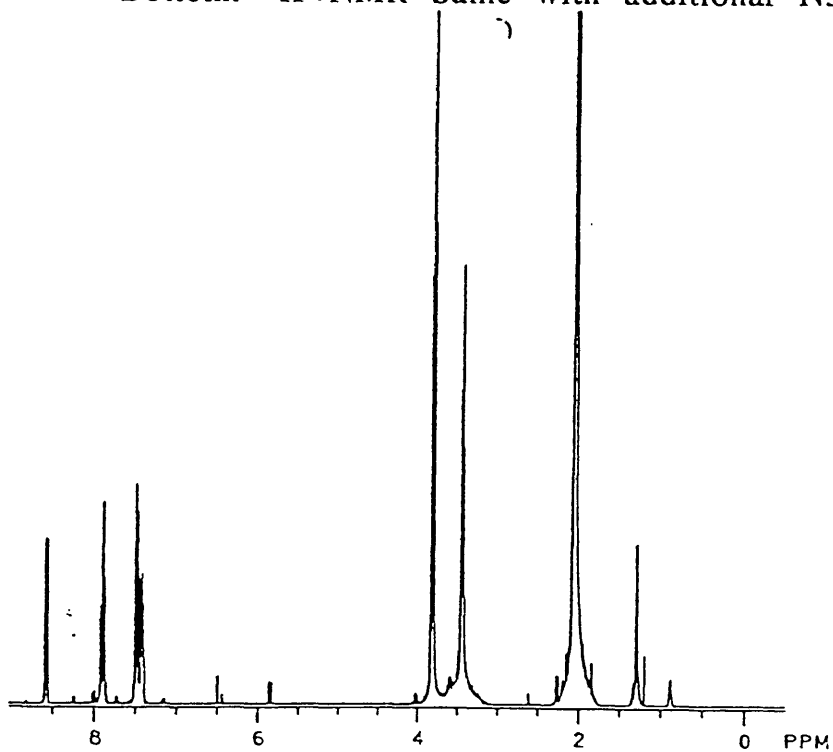
N 3·Hg·(ClO₄)₂
0.0 °C
Deuterated Acetone
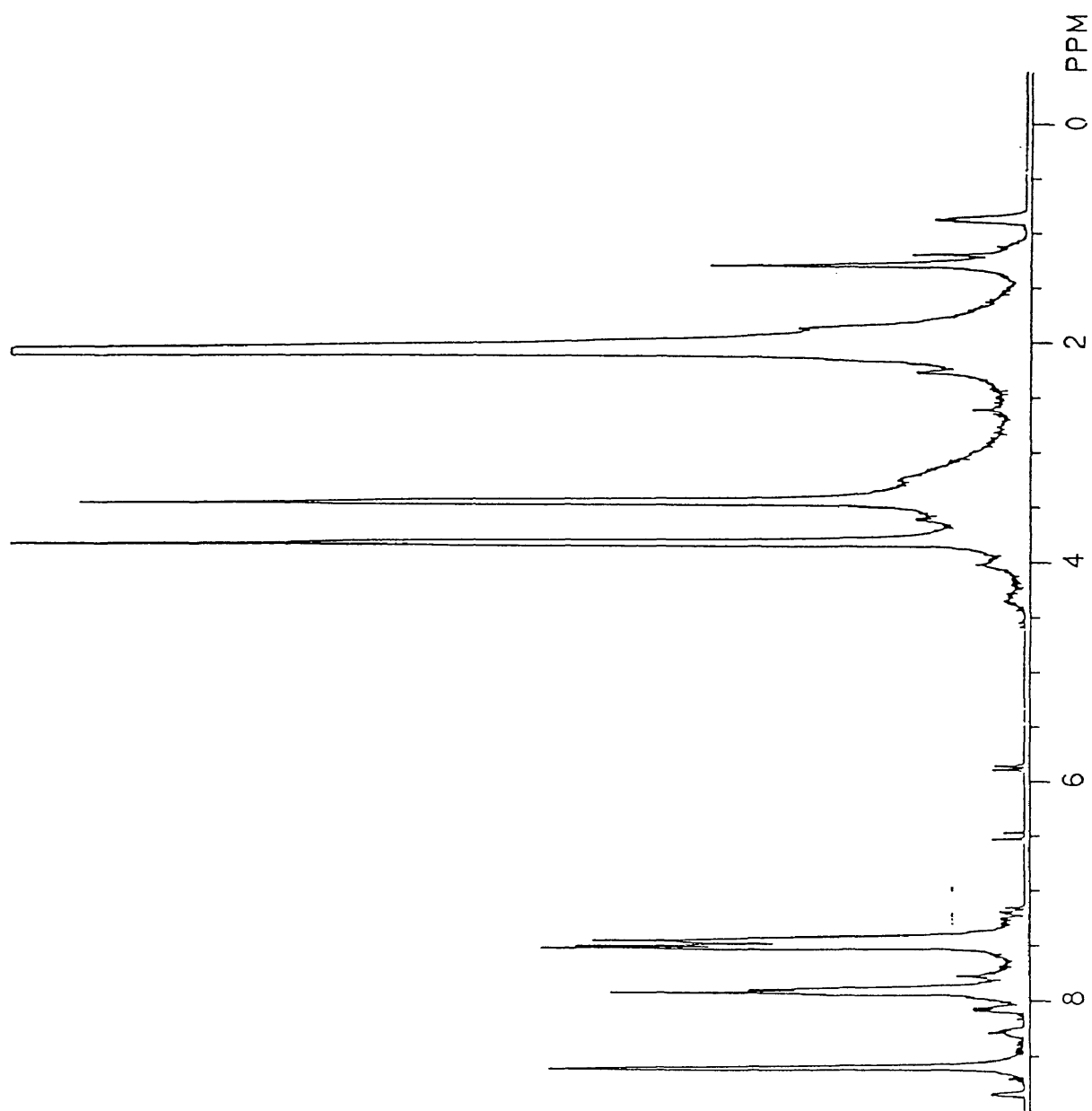
N 3·Hg·(ClO₄)₂
-20.0 °C
Deuterated Acetone
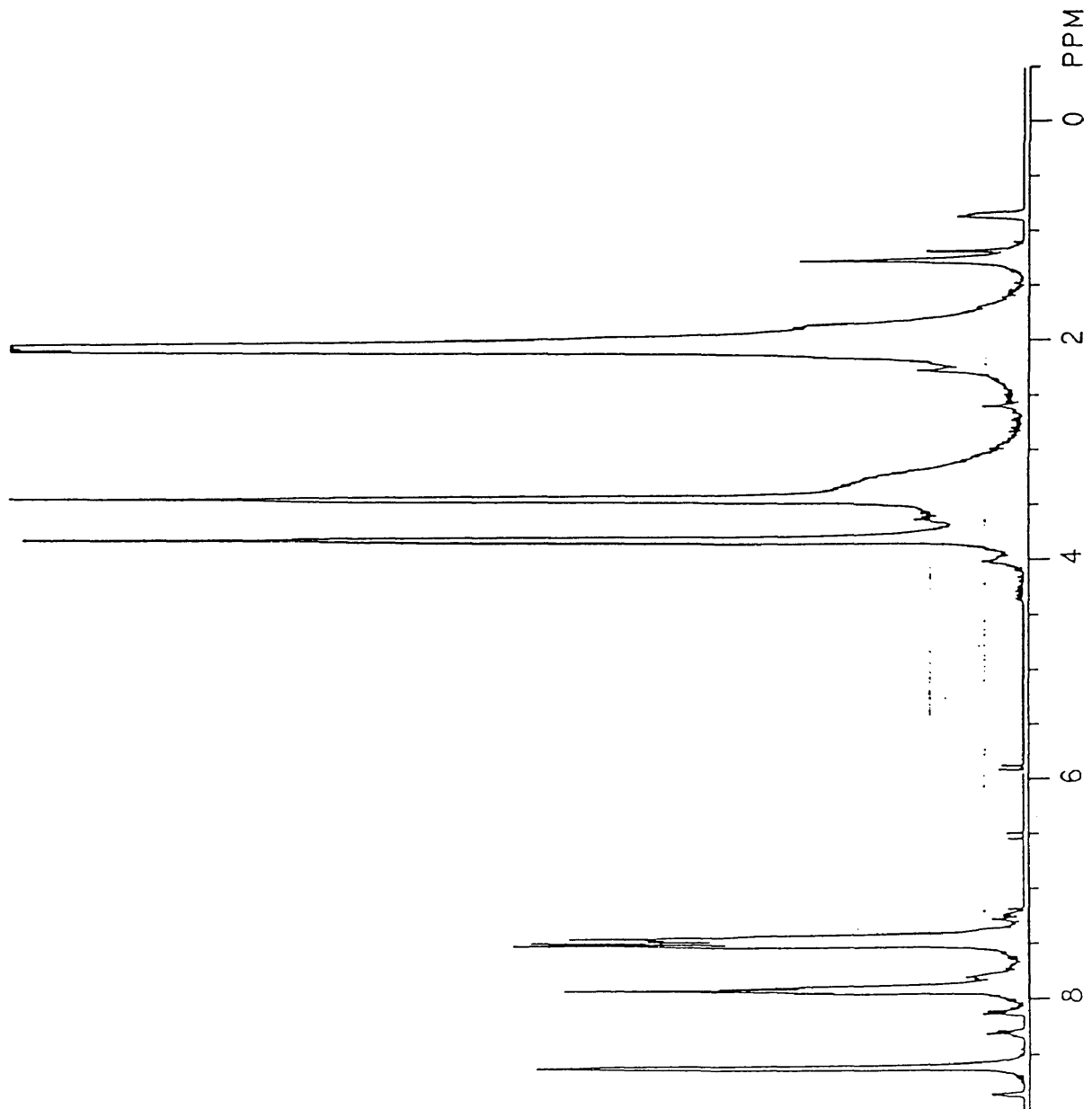
N 3·Hg·(ClO4)2

-40.0 °C

Deuterated   Acetone
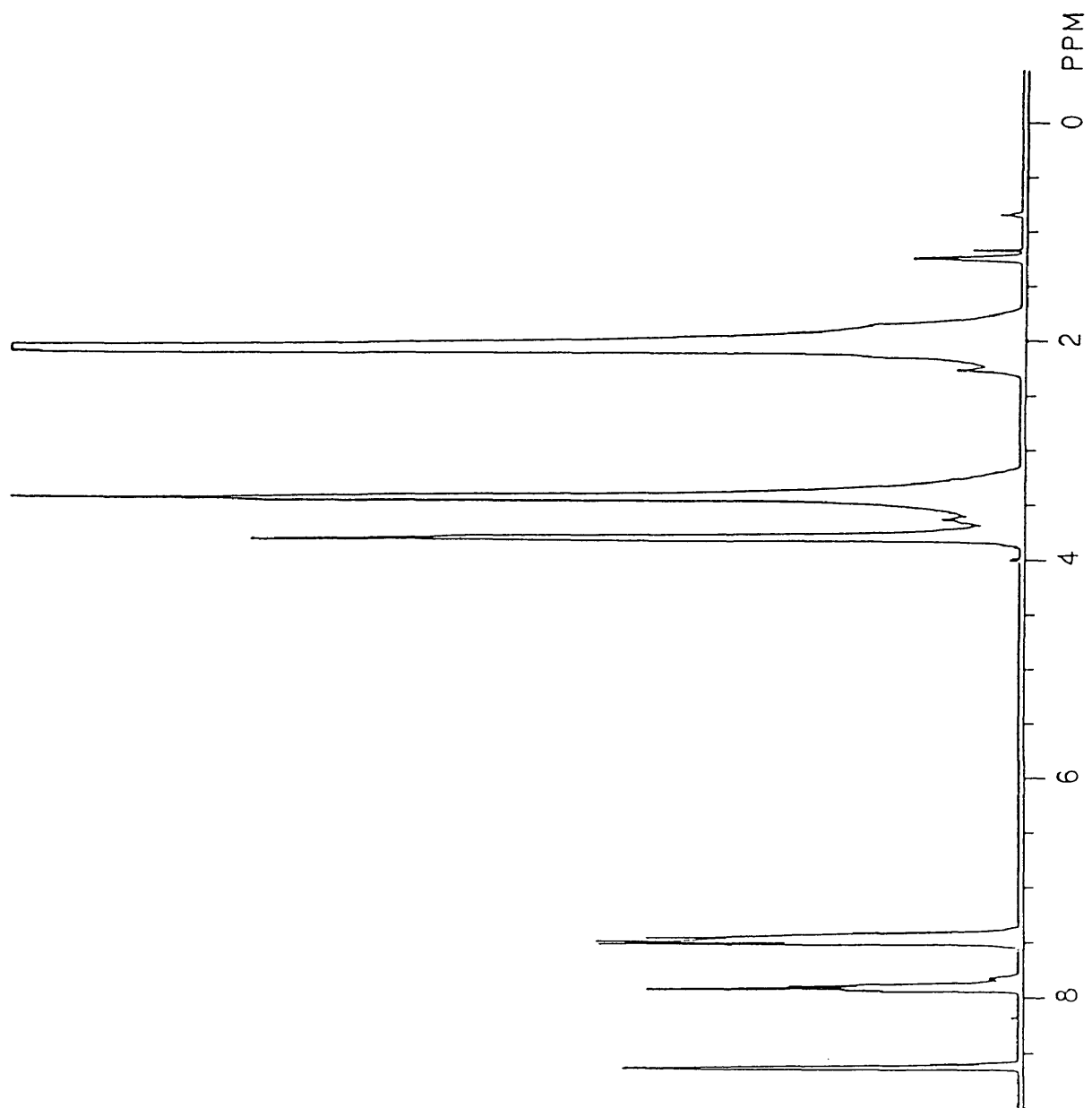
$N 3 \cdot H g \cdot (ClO_4)_2$

-50.0 °C

Deuterated   Acetone
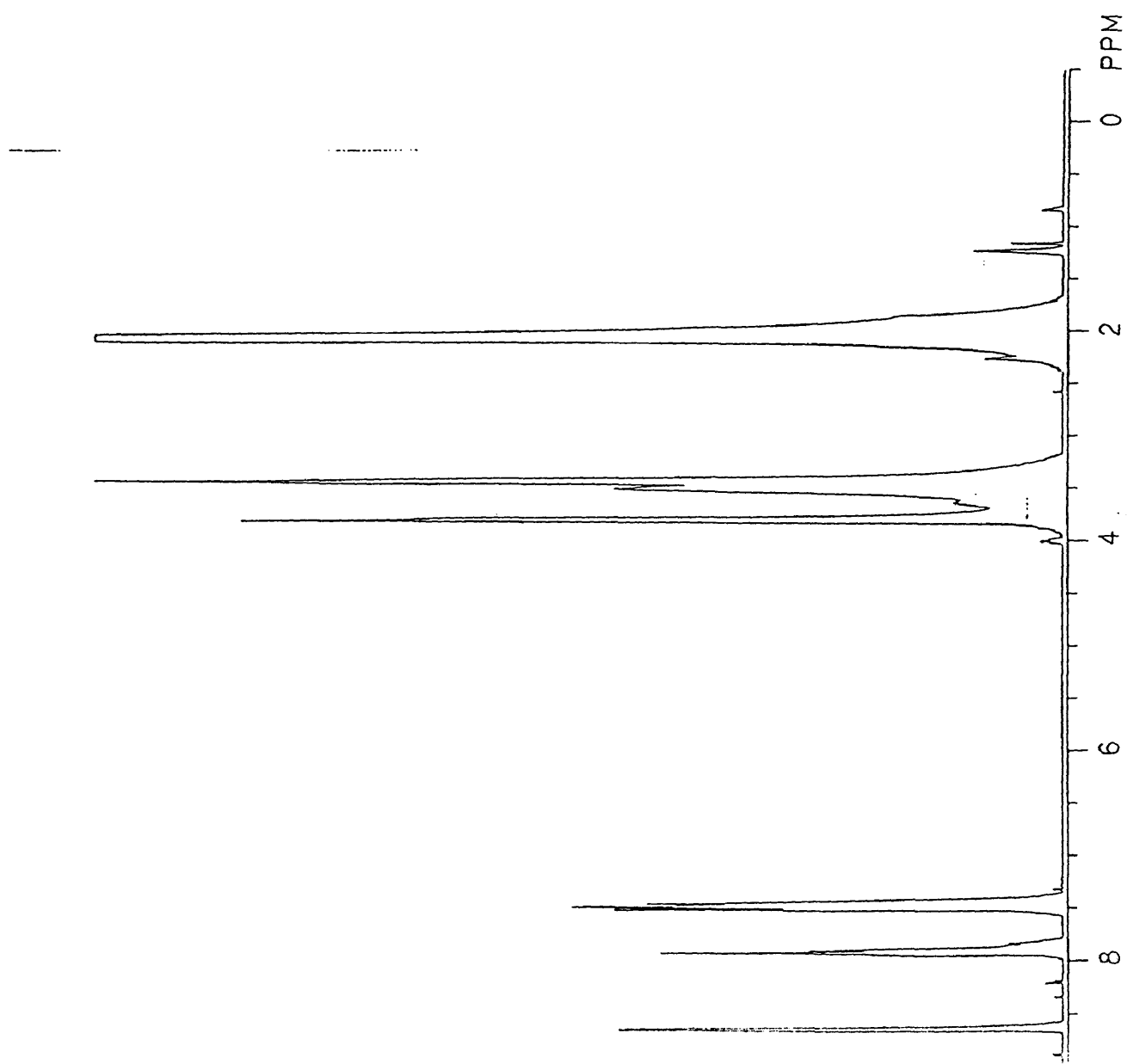
N 3·Hg·(ClO₄)₂
-60.0 °C
Deuterated Acetone
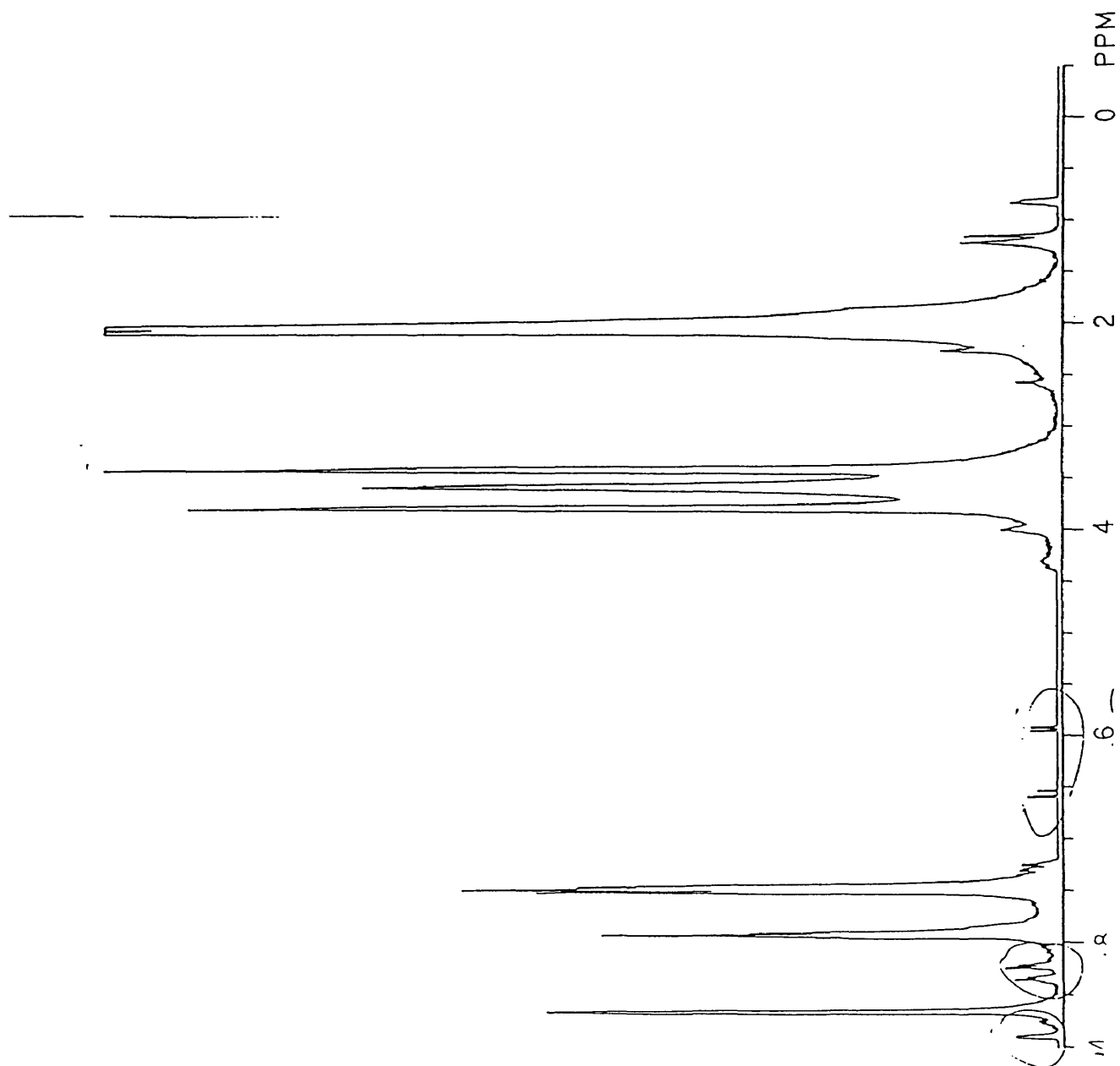
N 3·Hg·(ClO$_4$)$_2$

-70.0 °C

Deuterated Acetone
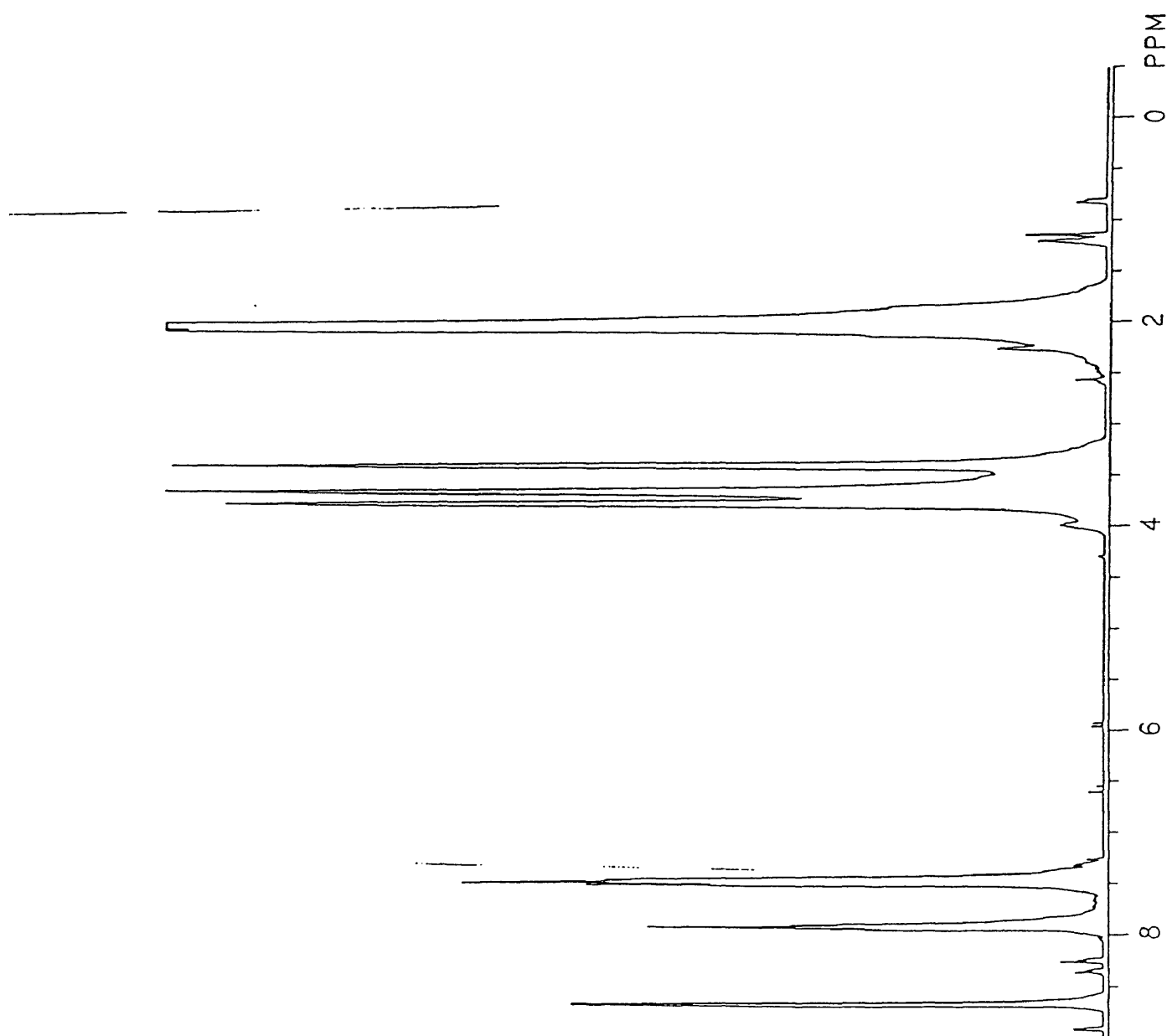
N 3·Hg·(ClO₄)₂
-80.0 °C
Deuterated Acetone
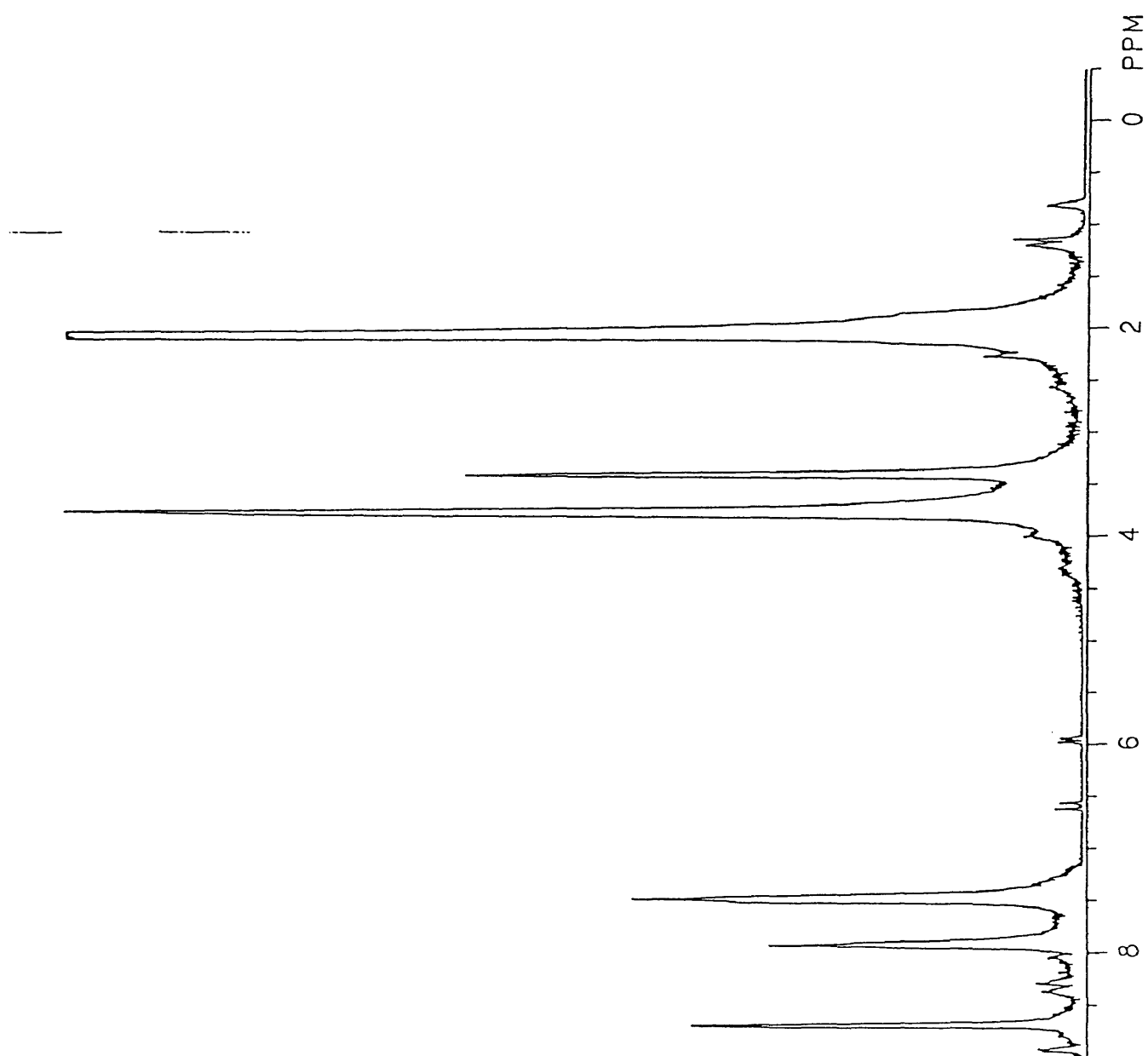
$$N\ 3 \cdot Hg \cdot (ClO_4)_2$$
-90.0 °C
Deuterated   Acetone
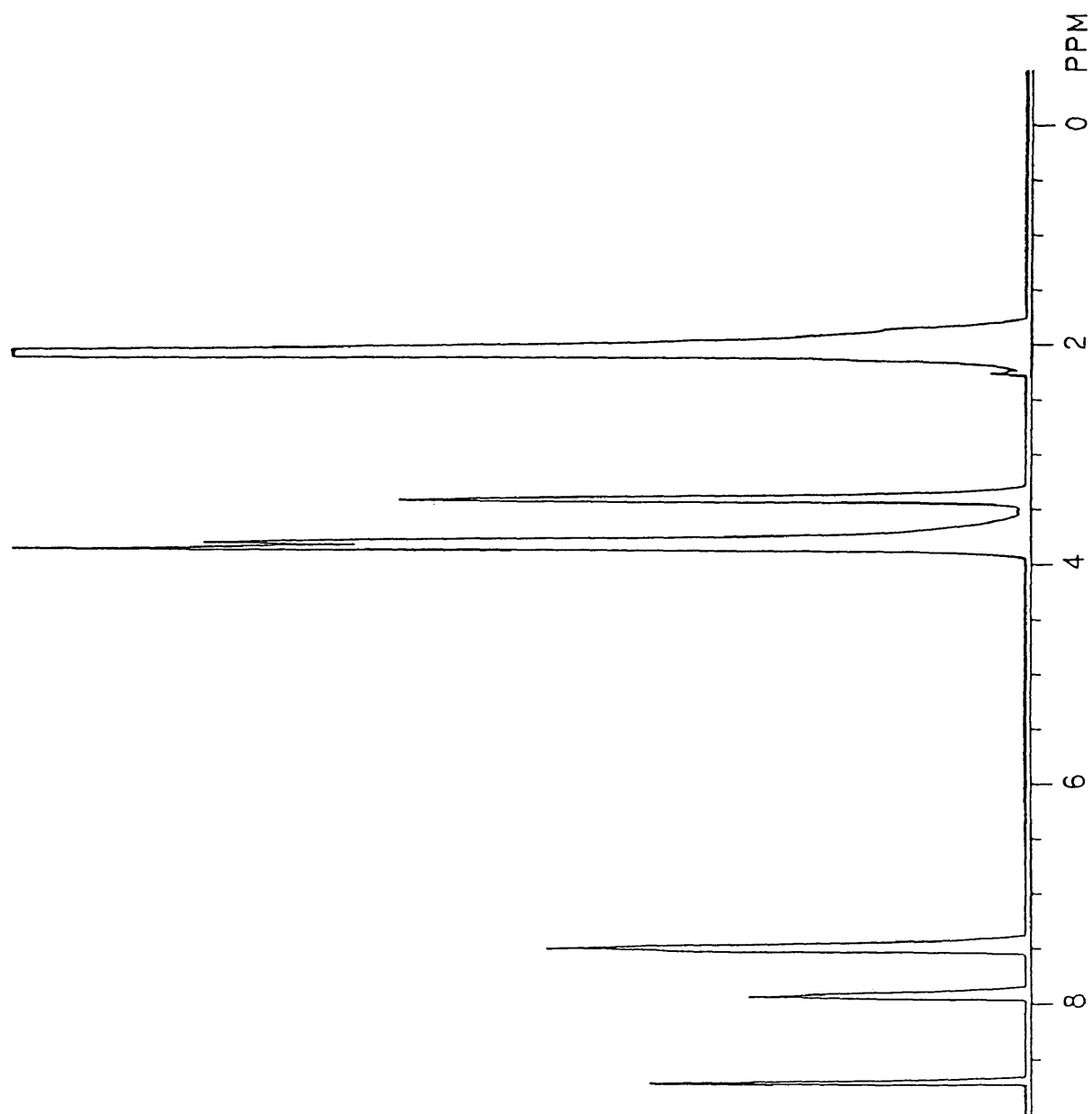
N 3·Hg·I2
0.0 °C
Deuterated   Acetone
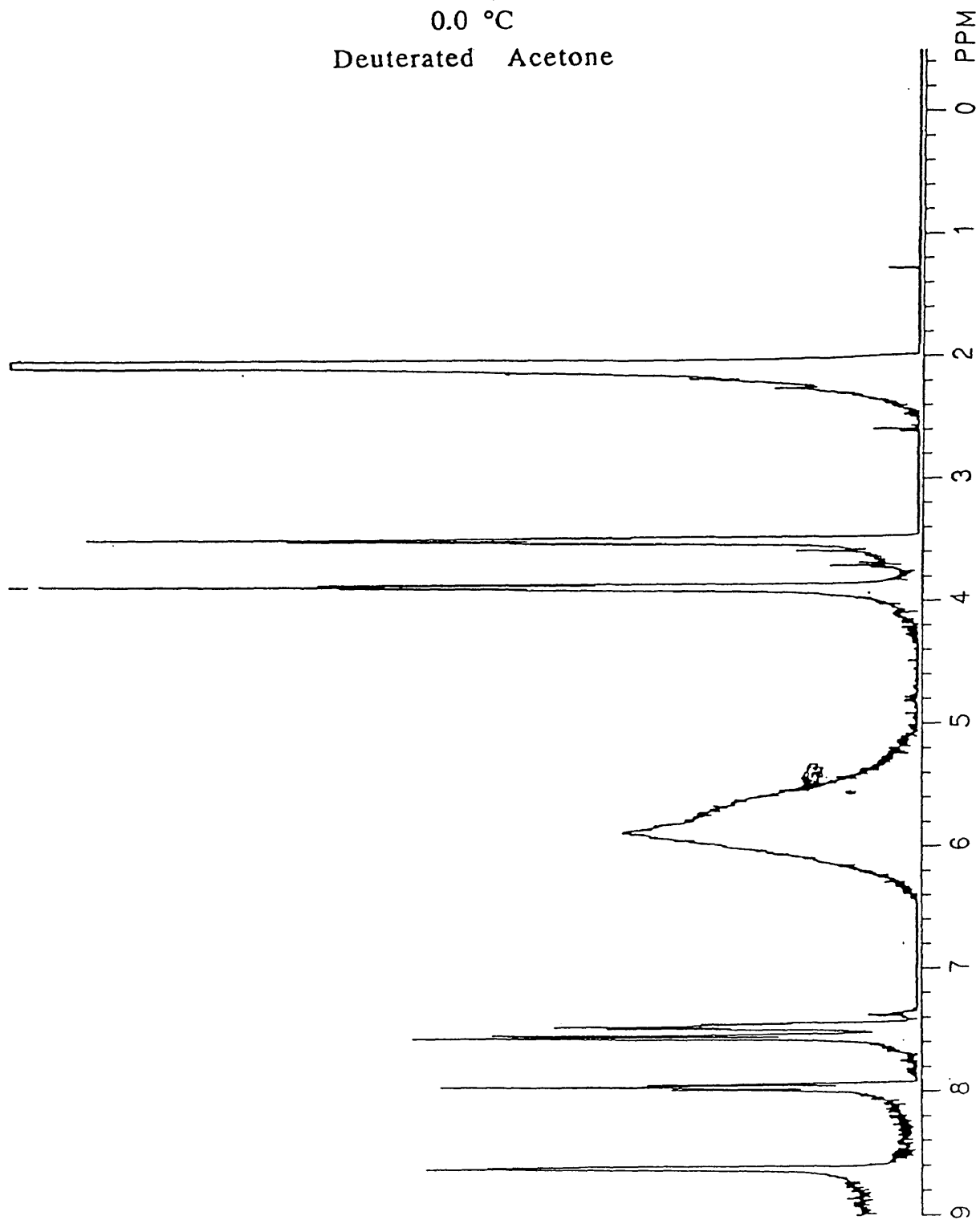
N 3•Hg•I₂
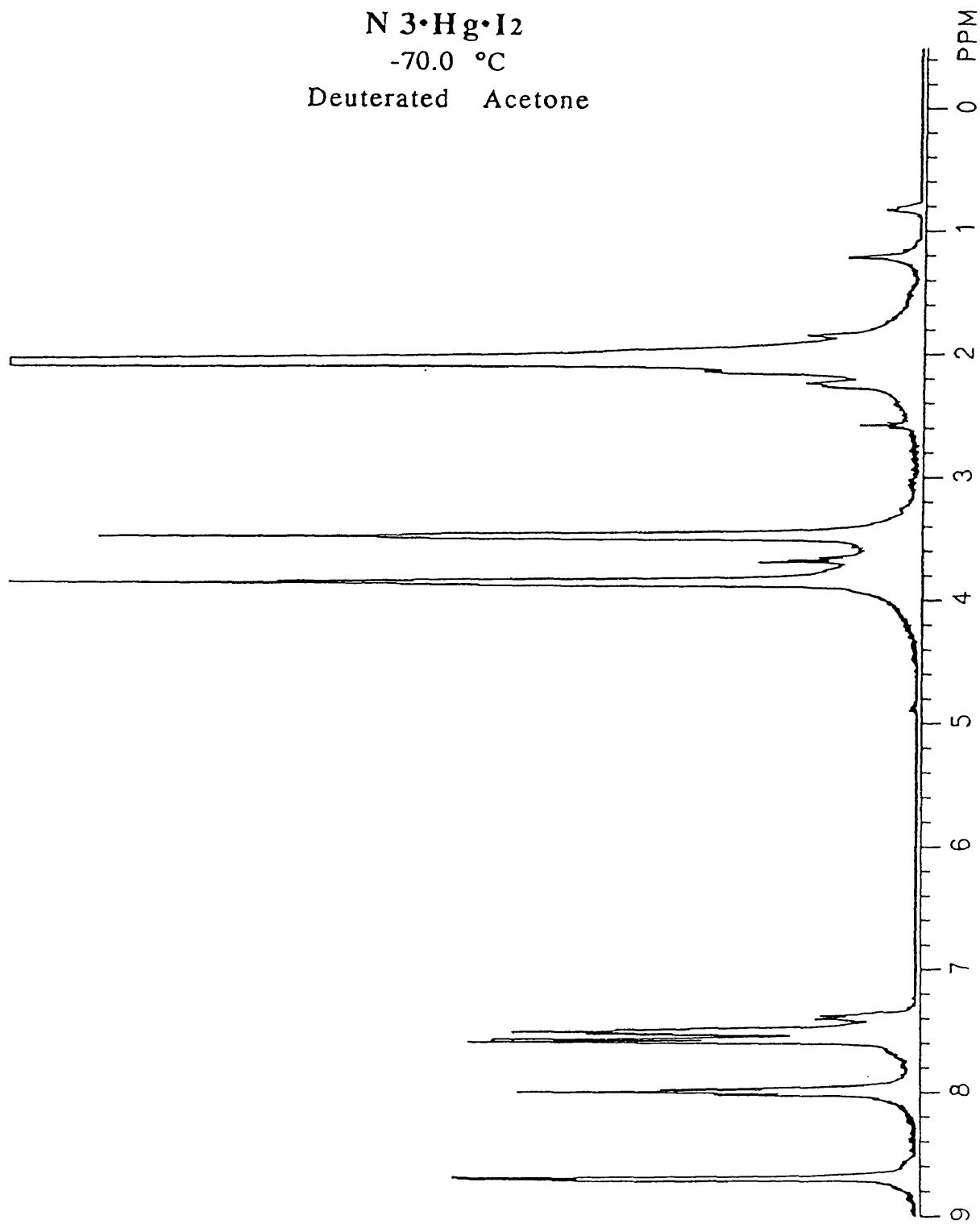## -40.0 °C
Deuterated Acetone
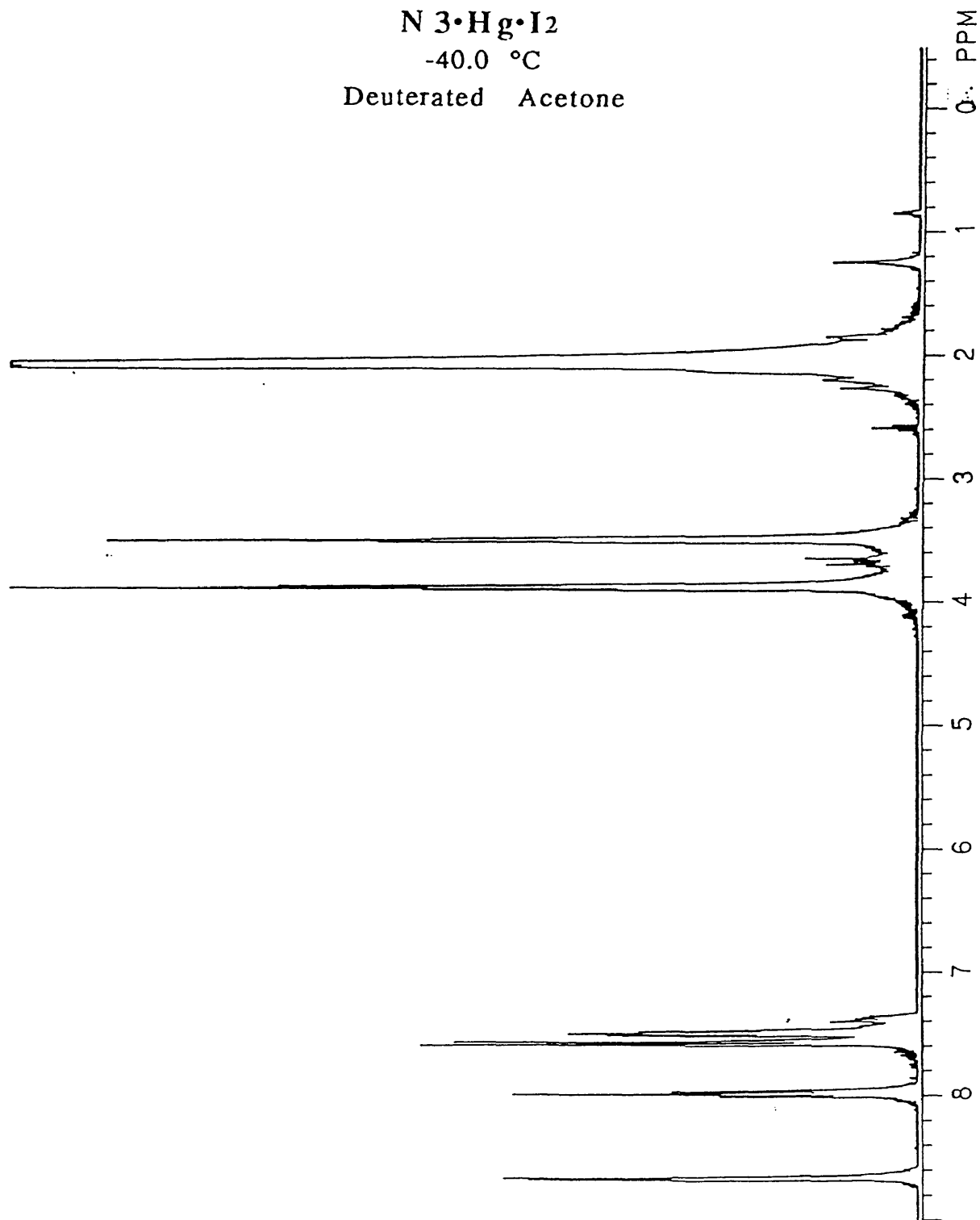
N 3·Hg·I₂
-50.0 °C
Deuterated Acetone
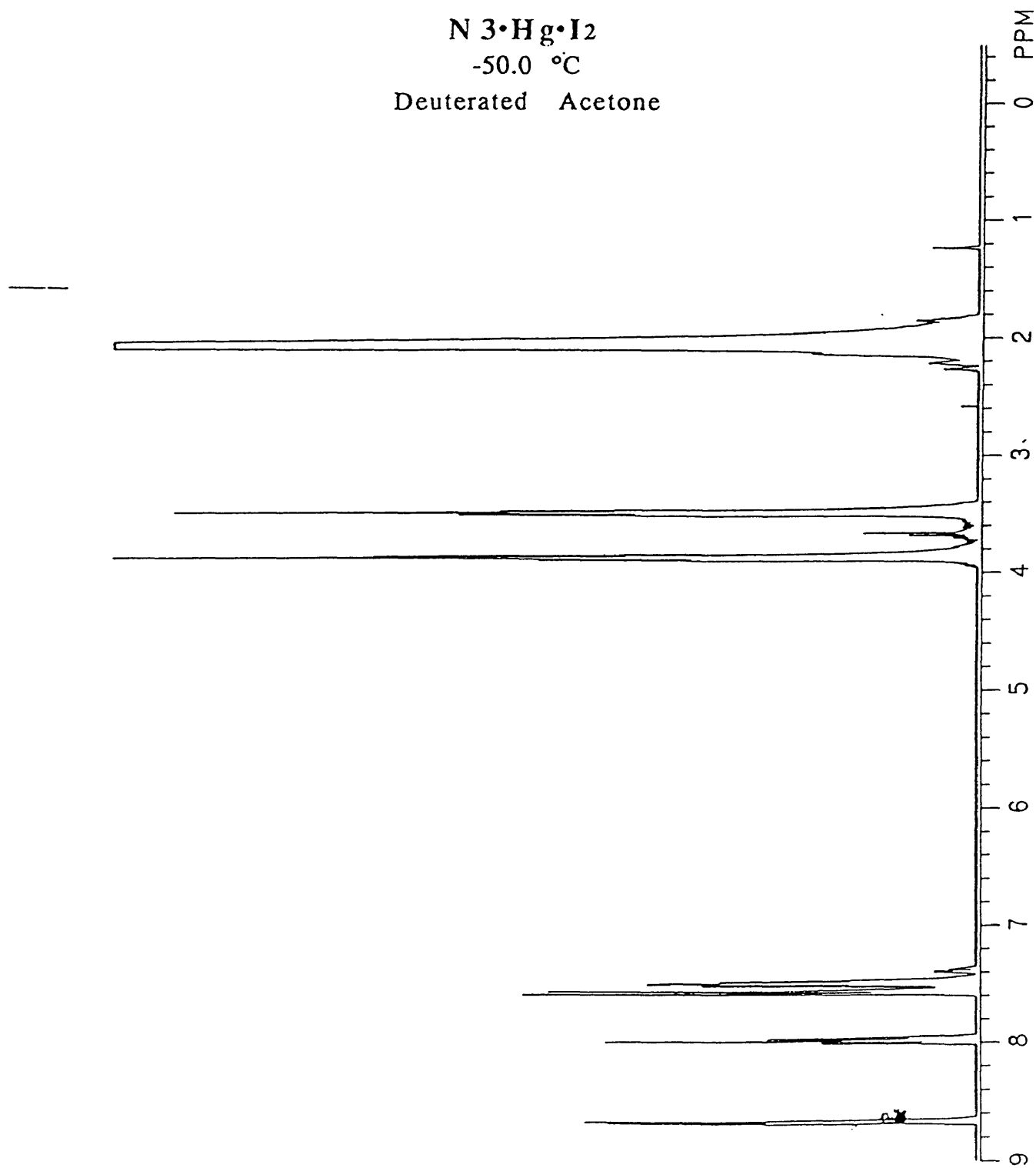
N 3·Hg·I₂
-70.0 °C
Deuterated   Acetone

N 3•Hg•(ClO₄)₂ + N3
-90.0 °C
Deuterated Acetone
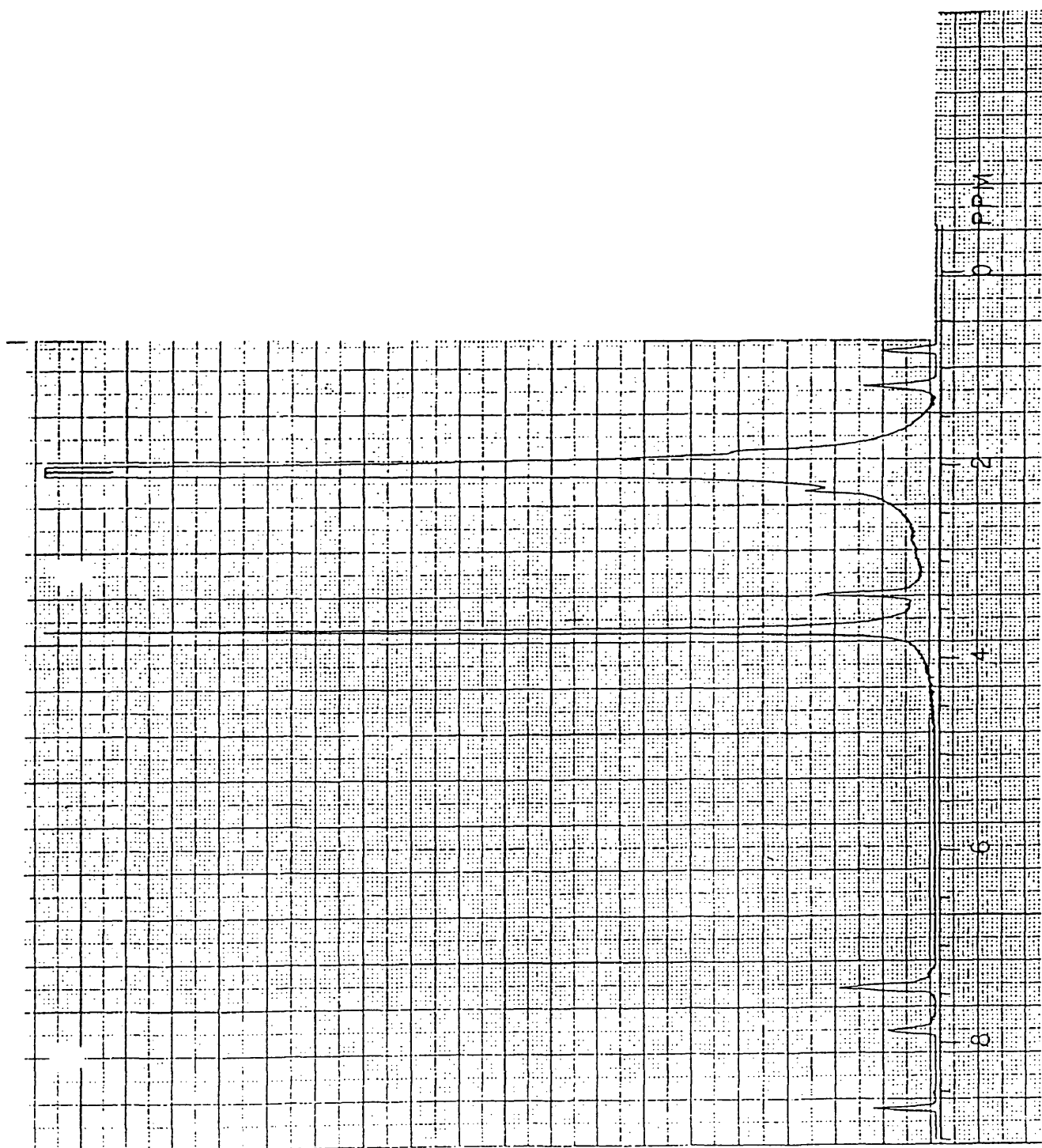
REFERENCES

Chapter One

1) Hawking, Stephen W. *A Brief History of Time*; Bantam Books: Toronto, 1988; p. 171.

2) Zumdahl, Stephen S. *Chemistry, 2nd ed.*; Le Quesne, Mary, Ed.; D.C. Heath: Lexington, MA, 1989, p. 1023.

3) Sudmeier, James L.; and Perkins, Thomas G. *J. Am. Chem. Soc. Comm.* **1977**, 99 (23), 1701-1702.

4) Moore, Melissa J.; Distefano, Mark D.; Zydowsky, Lynne D.; Cummings, Richard T.; and Walsh Christopher T. *Acc. Chem. Res.* **1990**, 23 (9), 301-308.

5) Sanders, Jeremy K.M.; and Hunter, Brian K. *Modern NMR Spectroscopy, 2nd ed.;* Oxford University Press: Oxford, 1993; p. 1.

6) Robert, Jan M.; and Rabenstein, Dallas L. *Anal. Chem.* **1991**, 63 (23), 2674-2679.

7) Sanders, Jeremy K.M.; and Hunter, Brian K. *Modern NMR Spectroscopy, 2nd ed.*; Oxford University Press: Oxford, 1993; pp. 205-215.

8) Baleja, James D.; Pon, Richard T.; and Sykes, Brian D. *Biochem.* **1990**, 29 (20), 4828-4839.

Chapter Two

1) Still, W. Clark, et. al. *J. Org. Chem.* **1978**, 43, 2923.

2) Brady, L.E.; Freifelder, M. and Stone, G.R. *J. Org. Chem.* **1961**, 26, 4757.

3) Karlin, Kenneth D.; Hayes, Jon C.; Hutchinson, John P.; Hyde, Jeffrey R.; and Zubieta, Jon. *Inorg. Chim. Acta.* **1982**, 64, L219-L220.

4) Che, Chi-Ming; Yam, Vivian Wing-Wah; and Mak, Thomas C. *J. Am. Chem. Soc.* **1990**, 112, 2284-2291.

5) Braz, G. I. *Zhur. Obshchei. Khim.* (Eng.) **1951**, 21, 688-693.

6) Dauben and McCoy. *J. Am. Chem. Soc.* **1959**, 81, 4863.

7) Bose, Ajay K.; and Lal, Bansi. *Tetrahedron Letters.* **1973**, 40, 3937-3940.

8) Cova, G.; Galizzioli, D.; Giusto, D.; and Marazzoni, F. *Inorg. Chim. Acta.* **1972**, 6 (2), 343-346.

Chapter Three

1) Brady, L.E.; Freifelder, M. and Stone, G.R. *J. Org. Chem.* **1961**, 26, 4757.

2) Silverstein, R.M.; Bassler, G. Clayton; and Morill, Terence C. *Spectrometric Identification of Organic Compounds, 5th ed.;* John Wiley and Sons: New York, 1991.

3) ^{13}C *NMR Spectroscopy of Organic Compounds.* pp. 322-325.

4) Che, Chi-Ming; Yam, Vivian Wing-Wah; and Mak, Thomas C. *J. Am. Chem. Soc.* **1990**, 112, 2284-2291.

Appendix A

1) Sanders, Jeremy K.; and Hunter, Brian K. *Modern NMR Spectroscopy, 2nd ed.*;
   Oxford University Press: Oxford, 1993.

2) Silverstein, R.M.; Bassler, G. Clayton; and Morill, Terence C.
   Spectrometric Identification of Organic Compounds; *5th ed.*
   John Wiley and Sons: New York, 1991.

3) Solomons, T.W. Graham. *Organic Chemistry, 4th ed.*; John Wiley
   and Sons: New York, 1988.

4) Robert, Jan M.; and Rabenstein, Dallas L. *Anal. Chem.* **1991**, 63,
   2674-2679.

VITA

Sharon Rosemary Fitzhenry

Born in Cheektawaga, New York, July 17, 1971. Graduated from Foxboro High School in that city, May 1989; B.S. in Chemistry, The College of William and Mary, May, 1993. M.A. candidate, The College of William and Mary, 1993-1995, with a concentration in Chemistry.